UNIVERSIDADE DE SÃO PAULO

INSTITUTO DE FÍSICA
CAIXA POSTAL 20516
01000 - SÃO PAULO - SP
BRASIL

publicações

IFUSP/P - 404

PHOTONEUTRON CROSS SECTIONS

by

E. Wolynec, A.R.V. Martinez, P. Gouffon,
Y. Miyao, V.A. Serrão and M.N. Martins

Instituto de Física, Universidade de São Paulo

Maio/1983

PHOTONEUTRON CROSS SECTIONS

E. Wolynec, A.R.V. Martinez, P. Gouffon,
Y. Miyao, V.A. Serrão and M.N. Martins

Universidade de São Paulo - Instituto de
Física, São Paulo, S.P., Brazil.

ABSTRACT

The differences between the Saclay and Livermore photoneutron cross sections are discussed. It is shown that the differences between the Saclay and Livermore (γ,n) and $(\gamma,2n)$ cross sections arise from the neutron multiplicity sorting.

1. INTRODUCTION

In the last 20 years, photoneutron cross sections have been measured for many nuclei using monoenergetic photons. Most of this work was carried out by two laboratories: Saclay and Livermore. The available results are compiled in the "Atlas of Photoneutron Cross Sections obtained with Monoenergetic Photons"[1]. There is also in the literature a few review articles on the subject but none of these publications has addressed the problem of the differences between the measurements performed by Saclay and Livermore. In this paper we compare the Saclay and Livermore measurements for the nuclei listed in Table I.

The typical differences between Saclay and Livermore data are illustrated in Fig. 1, where the (γ,n) measurements from Saclay and Livermore are shown. The results from Livermore are multiplied by 1.06 in order to show both cross sections in the same absolute scale. The cross sections are in good agreement up to the $(\gamma,2n)$ threshold. Above this energy there is an important difference: the Livermore cross section vanishes a few MeV above the $(\gamma,2n)$ threshold, in good agreement with the predictions of the statiscal model, while the Saclay cross section has a tail. In ref. 7), the observed tail of the Saclay cross section is interpreted as arising from fast

neutrons that would have escaped detection in the Livermore measurements, leading to the conclusion that for ^{159}Tb the contribution of the "direct effect" in the photoneutron cross section is $n_d = 23 \pm 4$ percent. In Table II the percentages of direct neutrons inferred by Saclay are given for several nuclei.

Figure 2 shows the $(\gamma,2n)$ cross sections from Saclay and Livermore. The $(\gamma,2n)$ cross sections differ in shape and magnitude, the Livermore one being much bigger. Eventhough up to the $(\gamma,2n)$ threshold the (γ,n) cross section from Livermore, $\sigma^L_{\gamma,n}$, and Saclay, $\sigma^S_{\gamma,n}$, differ by only 6 percent in the absolute scale, their integrated cross sections up to 28 MeV are 1413 and 1936 MeV.mb, respectively. While the integrated (γ,n) cross section from Saclay is 37% bigger than the Livermore result, their integrated $(\gamma,2n)$ cross section is 47% smaller.

2. ANALYSIS OF THE PHOTONEUTRON DATA

In order to understand these differences we reconstructed the total neutron measurements from Saclay and Livermore:

$$\sigma_{\gamma,tn} = \sigma_{\gamma,n} + 2\sigma_{\gamma,2n} + 3\sigma_{\gamma,3n} \qquad (1)$$

Since $\sigma_{\gamma,tn}$ is the cross section measured and the (γ,n) and $(\gamma,2n)$ cross sections are obtained by neutron multiplicity

sorting, it is important to compare $\sigma^{S}_{\gamma,tn}$ and $\sigma^{L}_{\gamma,tn}$. This comparison has not been discussed in the literature . Figure 3 shows $\sigma_{\gamma,tn}$ from Saclay and Livermore for ^{159}Tb. In figure 4 the ratio $r = \sigma^{S}_{\gamma,tn}/\sigma^{L}_{\gamma,tn}$ is shown. The ratio is reasonably constant and the least squares fit of a constant yields the value $r = 1.062 \pm 0.011$. In order to compute r we interpolated $\sigma^{S}_{\gamma,tn}$ and $\sigma^{L}_{\gamma,tn}$, since their data points are not at the same photon enegies. One important conclusion can be derived from figure 3: both laboratories are detecting the same number of neutrons for all photon energies. If there were fast neutrons escaping detection in the Livermore measurements above 20 MeV, r should increase above this energy. The value of the constant r is the difference in the absolute scale of both measurements. Figure 4 shows $\sigma^{L}_{\gamma,tn}$ multiplied by 1.06 and $\sigma^{S}_{\gamma,tn}$, just to illustrate the good agreement between them, when they are plotted at the same absolute scale.

Since both Laboratories agree as to the total number of neutrons detected, the differences in their (γ,n) and $(\gamma,2n)$ cross sections arise from the separation of the total counts into (γ,n) and $(\gamma,2n)$ events (neutron multiplicity sorting).

If we assume that the excess (γ,n) cross section in the Saclay measurement is due to $(\gamma,2n)$ events interpreted as two (γ,n) events, that is, if we compute:

$$\sigma^{S*}_{\gamma,2n} = \sigma^{S}_{\gamma,2n} + \frac{1}{2}\,(\sigma^{S}_{\gamma,n} - 1.06\sigma^{L}_{\gamma,n}) \qquad (2)$$

we obtain for $\sigma^{S*}_{\gamma,2n}$ the solid line shown in figure 5. The modified $\sigma_{\gamma,2n}$ cross section from Saclay agrees well with the $(\gamma,2n)$ cross section from Livermore multiplied by 1.06 (data points).

The same analysis carried out for ^{159}Tb was repeated for the nuclei listed in Table I. The results obtained for $\sigma_{\gamma,tn}$ are shown in part a) of figures 6 to 17, where the solid line represents the Saclay data and the experimental points are from Livermore.

The ratio $\sigma^{S}_{\gamma,tn}/\sigma^{L}_{\gamma,tn}$ is shown in part b) of figures 6 to 17. In order to calculate this ratio, the Saclay and Livermore data were interpolated to get both cross sections at the same photon energies. The energy interval, int, used in the interpolation is given in each figure. The solid line in each figure results from the least squares fit of a constant to the ratio. For ^{118}Sn, ^{120}Sn, ^{165}Ho and ^{181}Ta, figures 9, 10, 14 and 15, the fitting of a constant is not statistically acceptable, but a comparison between $\sigma_{\gamma,tn}$ from Livermore and Saclay indicates a displacement in the energy scale, because the peaks do not coincide in energy (see as an example figure 14-a) for ^{165}Ho). The ratio $\sigma^{S}_{\gamma,tn}/\sigma^{L}_{\gamma,tn}$ was also calculated with a variable e-

nergy displacement d. The displacement that yields a minimum of the χ^2 for fitting a constant to the ratio is chosen. Figures 18 to 23 show the data from Saclay and Livermore, with the Livermore data displaced by d. The value of d is given in part a) of the figures for each nucleus. The displacement was negative in all cases, that is, the Livermore data was shifted to lower energies. The displacement of the energy scale of the Livermore data is arbitrary and, of course, the same results can be obtained if the Saclay energy scale is moved up in energy by the same amount. For the nuclei shown in figures 18 to 23, the displacement of the energy scale improves the agreement between the shapes of $\sigma_{\gamma,tn}$, that is, the peaks coincide in energy (compare, as an example, figures 14-a) and 21-a) for ^{165}Ho).

If we accept the displacement of the energy scale, we can conclude that for all nuclei analyzed here, the measurements from Saclay and Livermore are in good agreement as to the number of emitted neutrons versus the incident photon energy, apart from an overall normalization constant. The differences between their (γ,n) and $(\gamma,2n)$ cross sections arise from the neutron multiplicity sorting.

In order to compare the (γ,n) and $(\gamma,2n)$ cross sections from both laboratories in the same energy scale, the Livermore data shown in all figures c), d), e) and f) are multiplied by r.

In figures 6-c) to 23-c) we show again the $\sigma_{\gamma,tn}$ cross sections, just to illustrate the good agreement between them, when they are plotted at the same absolute scale.

In figures 6-d) to 23-d) and 6-e) to 23-e) the (γ,n) and $(\gamma,2n)$ cross sections from Livermore and Saclay are shown. Like for ^{159}Tb, above the $(\gamma,2n)$ threshold the (γ,n) cross sections from Saclay are always bigger than the corresponding Livermore cross sections and the $(\gamma,2n)$ cross sections from Saclay are always smaller than those from Livermore.

If the Saclay $(\gamma,2n)$ cross section is modified using equation (2), the resulting $\sigma^{S*}_{\gamma,2n}$ agree well with the Livermore $(\gamma,2n)$ cross sections, as shown in figures 6-f) to 23-f).

The analysis performed here shows that the differences in shape and magnitude in the (γ,n) and $(\gamma,2n)$ cross sections measured by Saclay and Livermore arise from the neutron multiplicity sorting. However, this analysis does not allow to conclude which set of data has the correct multiplicity sorting.

We have measurements of the (e,n) and (e,2n) cross sections for ^{181}Ta. The (e,tn) = (e,n) + 2(e,2n) cross section was measured by detecting the neutrons. The (e,n) cross section was also measured by radioactivity. The (e,2n) cross section is obtained without the use of neutron multiplicity sorting:

$$\sigma_{e,2n} = \frac{1}{2} (\sigma_{e,tn} - \sigma_{e,n}) \qquad (3)$$

These results, which will be the subject of a forthcoming publication, indicate that the neutron multiplicity sorting carried out by Livermore is correct.

3. CONCLUSIONS

We have shown that the differences between the measurements from Saclay and Livermore for the (γ,n) and $(\gamma,2n)$ cross sections in nuclei arise from neutron multiplicity sorting. If the Saclay multiplicity sorting is in error, as indicated by our measurements in ^{181}Ta, there are some important implications .

If the shapes of the (γ,n) and $(\gamma,2n)$ cross sections from Livermore are correct, the (γ,n) cross sections for medium and heavy nuclei are statistical in nature and there are no large percentages of directly emitted neutrons (~ 20 percent) as deduced from the Saclay results.

More recently Saclay has performed measurements of photoneutron cross sections for photon energies up to 140 MeV[17]. Using their neutron multiplicity sorting technique, they unfolded the measured $\sigma_{\gamma,tn}$ into $\sigma_{\gamma,xn}$ cross sections, where x goes from 1 to ~ 10, depending on the nucleus. From the unfolded partial cross sections, the photoabsorption cross section, $\sigma_{\gamma,Tot}$ was obtained:

$$\sigma_{\gamma,Tot} = \sum_{x=1}^{N} \sigma_{\gamma,xn} \qquad (4)$$

This cross section was in disagreement with the prediction of the modified quasideuteron model[18,19] and motivated Levinger to change one of the parameters of the model to fit the Saclay data[20]. If the Saclay multiplicity sorting is in error, the results obtained for $\sigma_{\gamma,Tot}$ are questionable.

TABLE I

Nuclei measured by Saclay (S) and Livermore (L).

Nucleus	$\int\sigma_{\gamma,n}(E_\gamma)dE_\gamma$ [a] (MeV.mb)		$\int\sigma_{\gamma,2n}(E_\gamma)dE_\gamma$ [a] (MeV.mb)		References
^{89}Y	1279	S	74	S	2
	960	L	99	L	3
^{115}I	1470	S	278	S	4
	1354	L	508	L	5
^{117}Sn	1334	S	220	S	4
	1380	L	476	L	5
^{118}Sn	1377	S	258	S	4
	1302	L	531	L	5
^{120}Sn	1371	S	399	S	4
	1389	L	673	L	5
^{124}Sn	1056	S	502	S	4
	1285	L	670	L	5
^{133}Cs	1828	S	328	S	4
	1475	L	503	L	6
^{159}Tb	1936	S	605	S	7
	1413	L	887	L	8
^{165}Ho	2090	S	766	S	7
	1735	L	744	L	9
^{181}Ta	2180	S	790	S	7
	1300	L	881	L	10
^{197}Au	2588	S	479	S	11
	2190	L	777	L	12
^{208}Pb	2731	S	328	S	11
	1776	L	860	L	13

a) From reference 1)

TABLE II

Percentage of direct neutrons obtained by Saclay.

Nucleus	n_d (%)	References
^{94}Mo	25 ± 7	14
^{96}Mo	15 ± 7	14
^{98}Mo	10 ± 7	14
^{100}Mo	11 ± 7	14
^{139}La	28 ± 5	7
^{140}Ce	12 ± 3	15
^{142}Ce	10 ± 3	15
Nat_{Sm}	10 ± 3	15
^{159}Tb	23 ± 4	7
^{165}Ho	23 ± 4	7
Nat_{Er}	11 ± 3	15
^{175}Lu	15 ± 3	15
^{181}Ta	22 ± 2	7
^{197}Au	20 ± 4	11
^{208}Pb	15 ± 4	11
^{238}U	14 ± 2	16

REFERENCES

1. Atlas of photoneutron cross section obtained with monoenergetic photons, Bicentennial Edition, Preprint UCRL-78482 , edited by B.L. Berman and, B.L. Berman, Rev. Mod. Phys. 47, 713 (1975).

2. A. Lepretre, H. Beil, R. Bergere, P. Carlos, A. Veyssiere and M. Sugawara, Nucl. Phys. A175, 609 (1971).

3. B.L. Berman, J.T. Caldwell, R.R. Harvey, M.A. Kelly, R.L. Bramblett and S.C. Fultz, Phys. Rev. 162, 1098 (1967).

4. A. Lepretre, H. Beil, R. Bergere, P. Carlos, A. Deminiac and A. Veyssiere , Nucl. Phys. A219, 39 (1974).

5. S.C. Fultz, B.L. Berman, J.T. Caldwell, R.L. Bramblett and M.A. Kelly, Phys. Rev. 186, 1255 (1969).

6. B.L. Berman, R.L. Bramblett, J.T. Caldwell, H.S. Davis, M. A. Kelly and S.C. Fultz, Phys. Rev. 177, 1745 (1969).

7. R.L. Bergere, H. Beil and A. Veyssiere, Nucl. Phys. A121, 463 (1968).

8. R.L. Bramblett, J.T. Caldwell, R.R. Harvey and S.C. Fultz, Phys. Rev. B133, 869 (1964).

9. B.L. Berman, M.A. Kelly, R.L. Bramblett, J.T. Caldwell , H.S. Davis and S.C. Fultz, Phys. Rev. 185, 1576 (1969).

10. R.L. Bramblett, J.T. Caldwell, G.F. Auchampaugh and S.C. Fultz, Phys. Rev. 129, 2723 (1963).

11. A. Veyssiere, H. Beil, R. Bergere, P. Carlos and A. Lepretre, Nucl. Phys. A159, 561 (1970).

12. S.C. Fultz, R.L. Bramblett, J.T. Caldwell and N.A. Kerr , Phys. Rev. 127, 1237 (1962).

13. R.R. Harvey, J.T. Caldwell, R.L. Bramblett and S.C. Fultz, Phys. Rev. B136, 126 (1964).

14. H. Beil, R. Bergere, P. Carlos, A. Lepretre, A. Deminiac and A. Veyssiere, Nucl. Phys. A227, 427 (1974).

15. R. Bergere, H. Beil, P. Carlos, and A. Veyssiere, Nucl. Phys. A133, 417 (1969).

16. A. Veyssiere, H. Beil, R. Bergere, P. Carlos, A. Lepretre and K. Kernbach, Nucl. Phys. A199, 45 (1973).

17. P.J. Carlos, Lecture Notes in Phys. 137, 168 (1981).

18. J.S. Levinger, Phys. Rev. 84, 43 (1951).

19. J.S. Levinger, Proc. Intern. Conf. Low and Intermediate Energy Electromagnetic Interactions (Academy of Sciences , USSR, Moscow, 1967) vol. 3, p. 411.

20. J.S. Levinger, Phys. Lett. 82B, 181 (1979).

FIGURE CAPTIONS

Fig. 1 - (γ,n) cross sections from Saclay (solid line) and Livermore (experimental points) for ^{159}Tb. The Livermore data is multiplied by 1.06 in order to show both measurements at the same absolute scale.

Fig. 2 - $(\gamma,2n)$ cross sections from Saclay (solid line) and Livermore (experimental points) for ^{159}Tb. The Livermore data is multiplied by 1.06 in order to show both measurements at the same absolute scale.

Fig. 3 - $\sigma_{\gamma,tn}$ from Saclay divided by $\sigma_{\gamma,tn}$ from Livermore . $\sigma_{\gamma,tn} = \sigma_{\gamma,n} + 2\sigma_{\gamma,2n} + 3\sigma_{\gamma,3n}$.

Fig. 4 - $\sigma_{\gamma,tn}$ from Livermore multiplied by 1.06 (experimental points) and $\sigma_{\gamma,tn}$ from Saclay (solid line). $\sigma_{\gamma,tn} = \sigma_{\gamma,n} + 2\sigma_{\gamma,2n} + 3\sigma_{\gamma,3n}$.

Fig. 5 - $\sigma_{\gamma,2n}$ from Livermore (experimental points) and the modified (see text) $\sigma_{\gamma,2n}$ from Saclay (solid line).

Figs. 6 to 17 - The solid line represents the Saclay data and the experimental points are from Livermore.

a) $\sigma_{\gamma,tn} = \sigma_{\gamma,n} + 2\sigma_{\gamma,2n} + 3\sigma_{\gamma,3n}$ from Saclay and Livermore.

b) $\sigma_{\gamma,tn}$ from Saclay divided by $\sigma_{\gamma,tn}$ from Livermore. The Saclay and Livermore data were interpolated in order to have both cross sections at the same photon energies. The energy interval, int, used in the interpolation is given in the figure. The solid line shows r, the value obtained by fitting a constant to the ratio.

c) $\sigma_{\gamma,tn}$ from Livermore multiplied by r and $\sigma_{\gamma,tn}$ from Saclay.

d) $\sigma_{\gamma,n}$ from Livermore multiplied by r and $\sigma_{\gamma,n}$ from Saclay.

e) $\sigma_{\gamma,2n}$ from Livermore multiplied by r and $\sigma_{\gamma,2n}$ from Saclay.

f) $\sigma_{\gamma,2n}$ from Livermore multiplied by r and the modified $\sigma_{\gamma,2n}$ from Saclay. $\sigma^{S*}_{\gamma,2n} = \sigma^{S}_{\gamma,2n} + \frac{1}{2}(\sigma^{S}_{\gamma,n} - r\sigma^{L}_{\gamma,n})$.

Figs. 18 to 23 - a) $\sigma_{\gamma,tn}$ from Saclay and Livermore. The energy scale of the Livermore data is displaced by d. The value of the displacement is given in the figure.

b), c), d), e) and f) - The same as for figures 1 to 12.

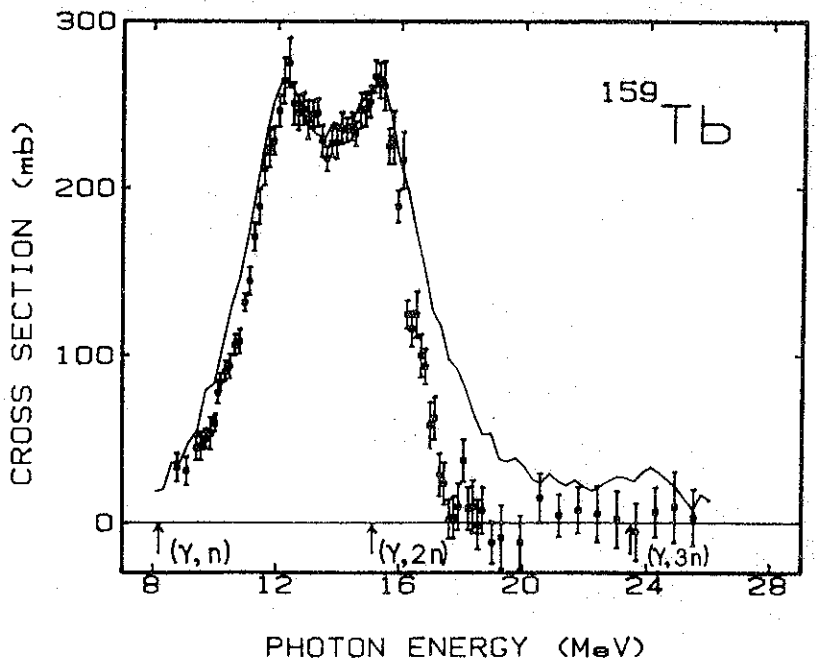

FIG. 1

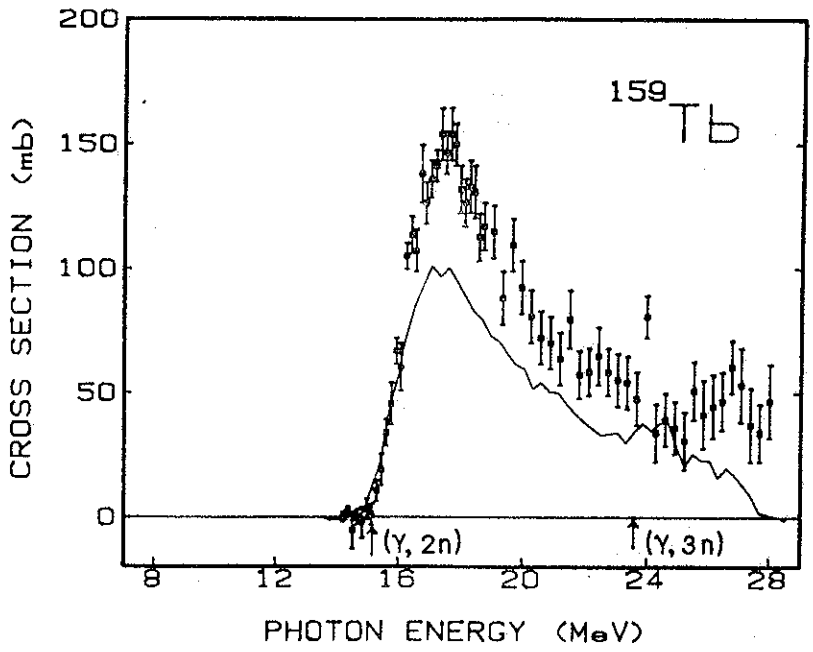

FIG. 2

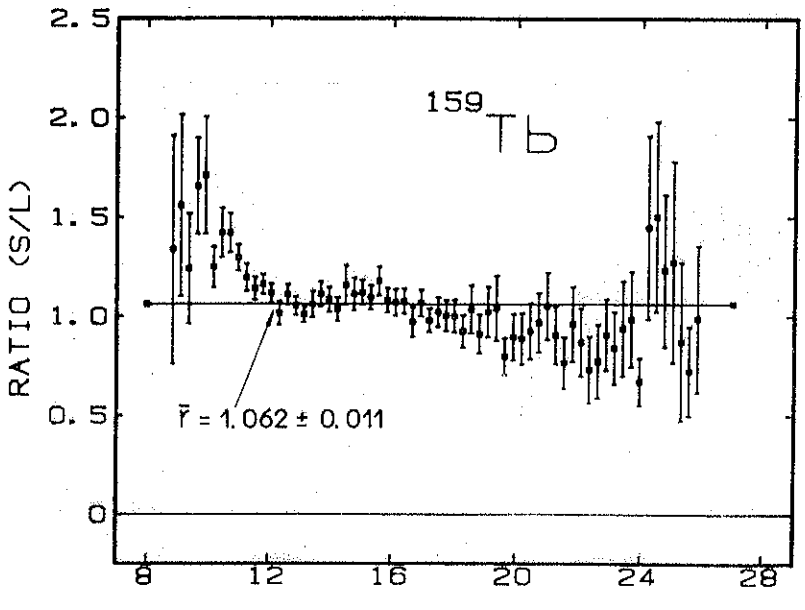

FIG. 3

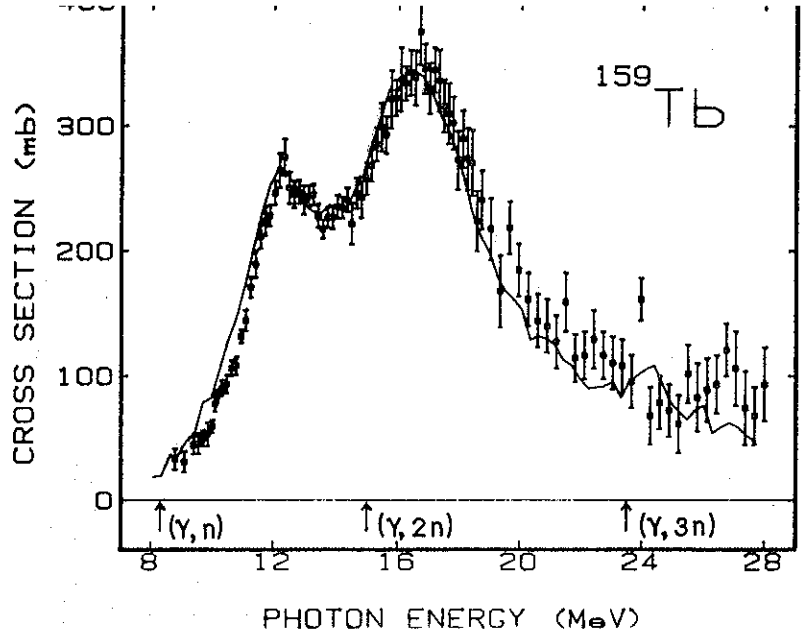
159Tb
CROSS SECTION (mb)
300
200
100
0
(γ, n)
(γ, 2n)
(γ, 3n)
8
12
16
20
24
28
PHOTON ENERGY (MeV)

FIG. 4

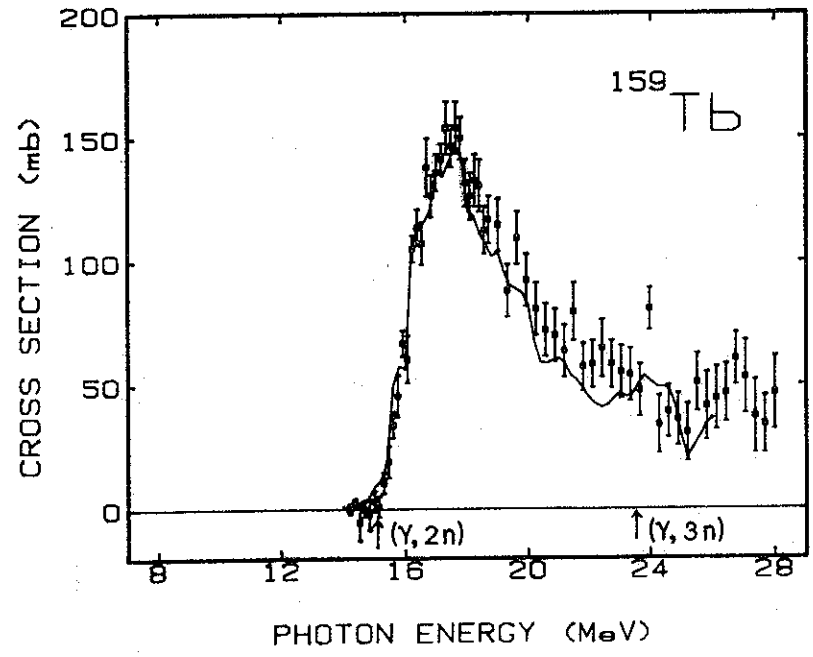
159Tb
CROSS SECTION (mb)
200
150
100
50
0
(γ, 2n)
(γ, 3n)
8
12
16
20
24
28
PHOTON ENERGY (MeV)

FIG. 5

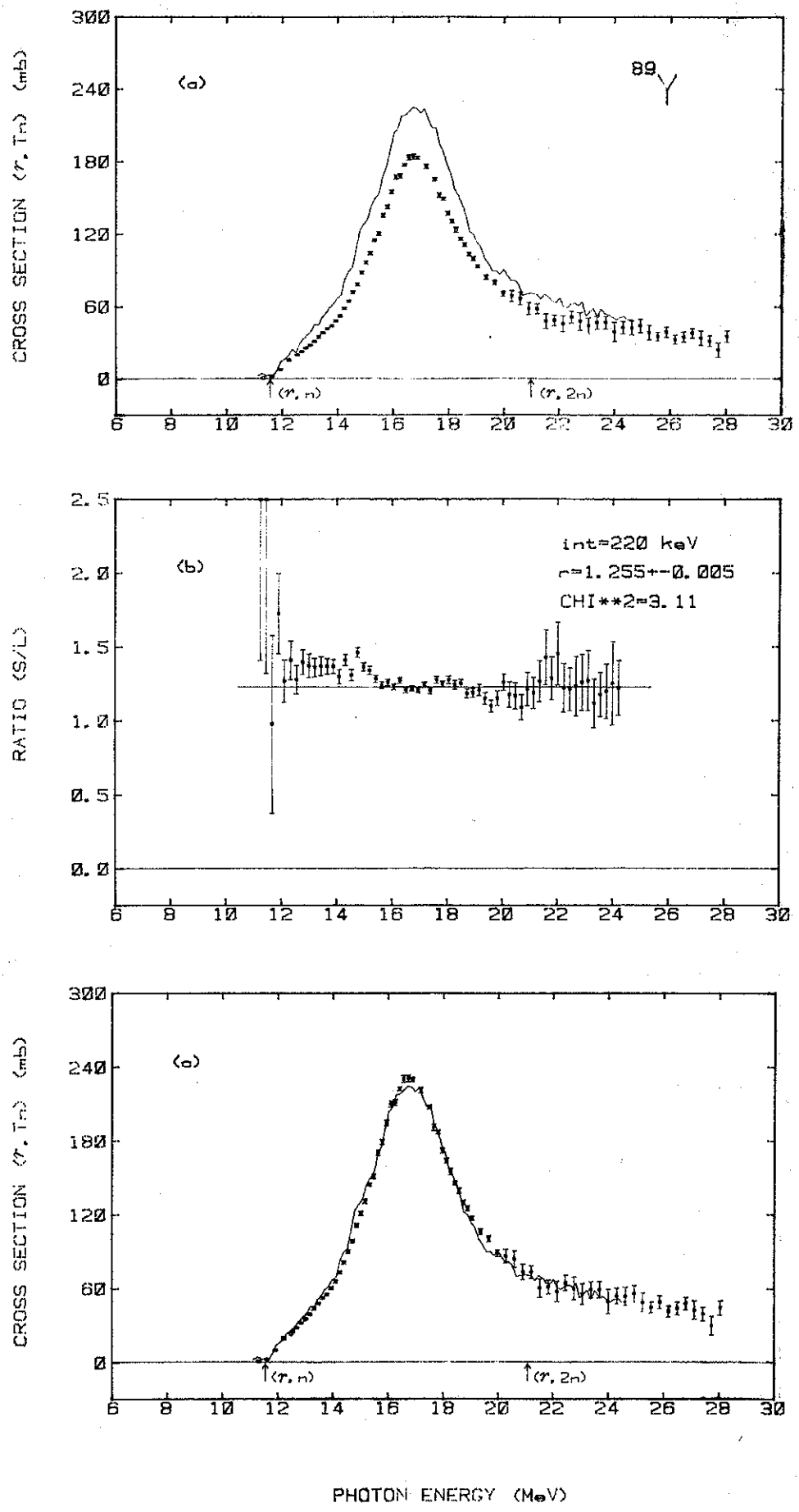
(a)
89Y
CROSS SECTION (γ, Tn) (mb)
(γ, n)
(γ, 2n)
(b)
int=220 keV
r=1.255+-0.005
CHI**2=3.11
RATIO (S/L)
PHOTON ENERGY (MeV)

FIG. 6

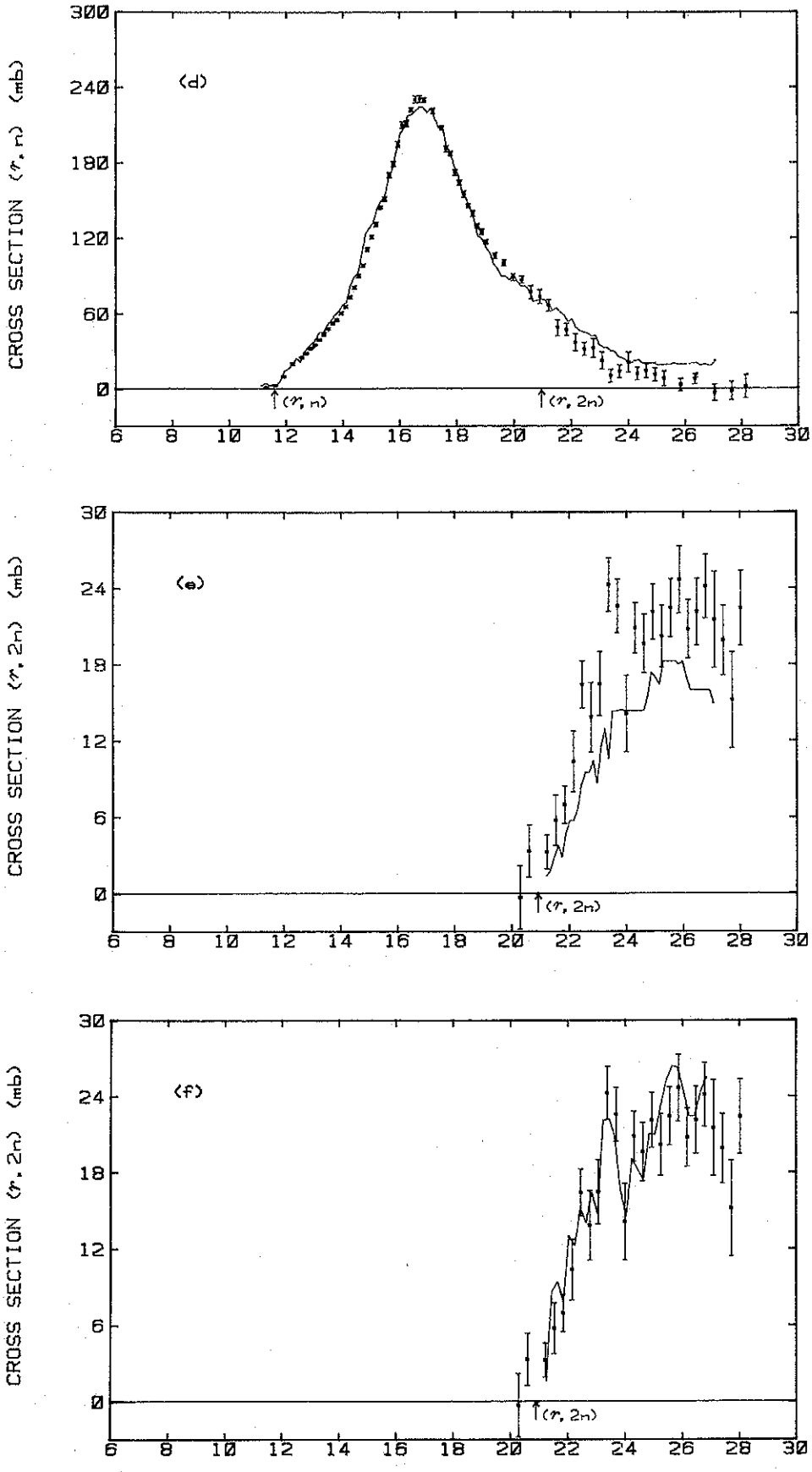
(d)
CROSS SECTION (γ, n) (mb)
300
240
180
120
60
0
(γ, n)
(γ, 2n)
6 8 10 12 14 16 18 20 22 24 26 28 30
(e)
CROSS SECTION (γ, 2n) (mb)
30
24
18
12
6
0
(γ, 2n)
6 8 10 12 14 16 18 20 22 24 26 28 30
(f)
CROSS SECTION (γ, 2n) (mb)
30
24
18
12
6
0
(γ, 2n)
6 8 10 12 14 16 18 20 22 24 26 28 30
PHOTON ENERGY (MeV)

FIG. 6

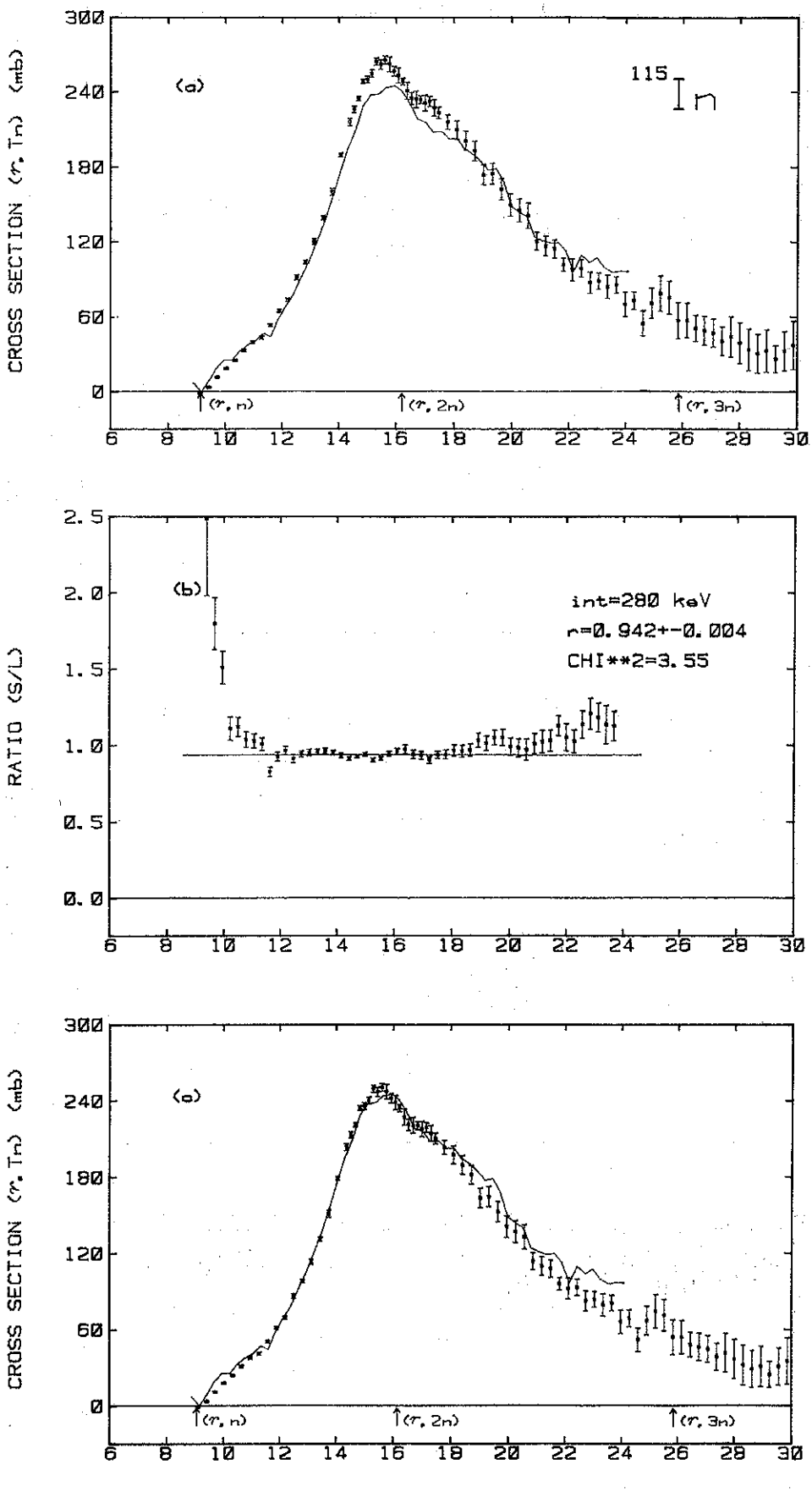
(a)
115 In
CROSS SECTION (γ, Tn) (mb)
(γ, n)
(γ, 2n)
(γ, 3n)
(b)
int=280 keV
r=0.942+-0.004
CHI**2=3.55
RATIO (S/L)
PHOTON ENERGY (MeV)

FIG. 7

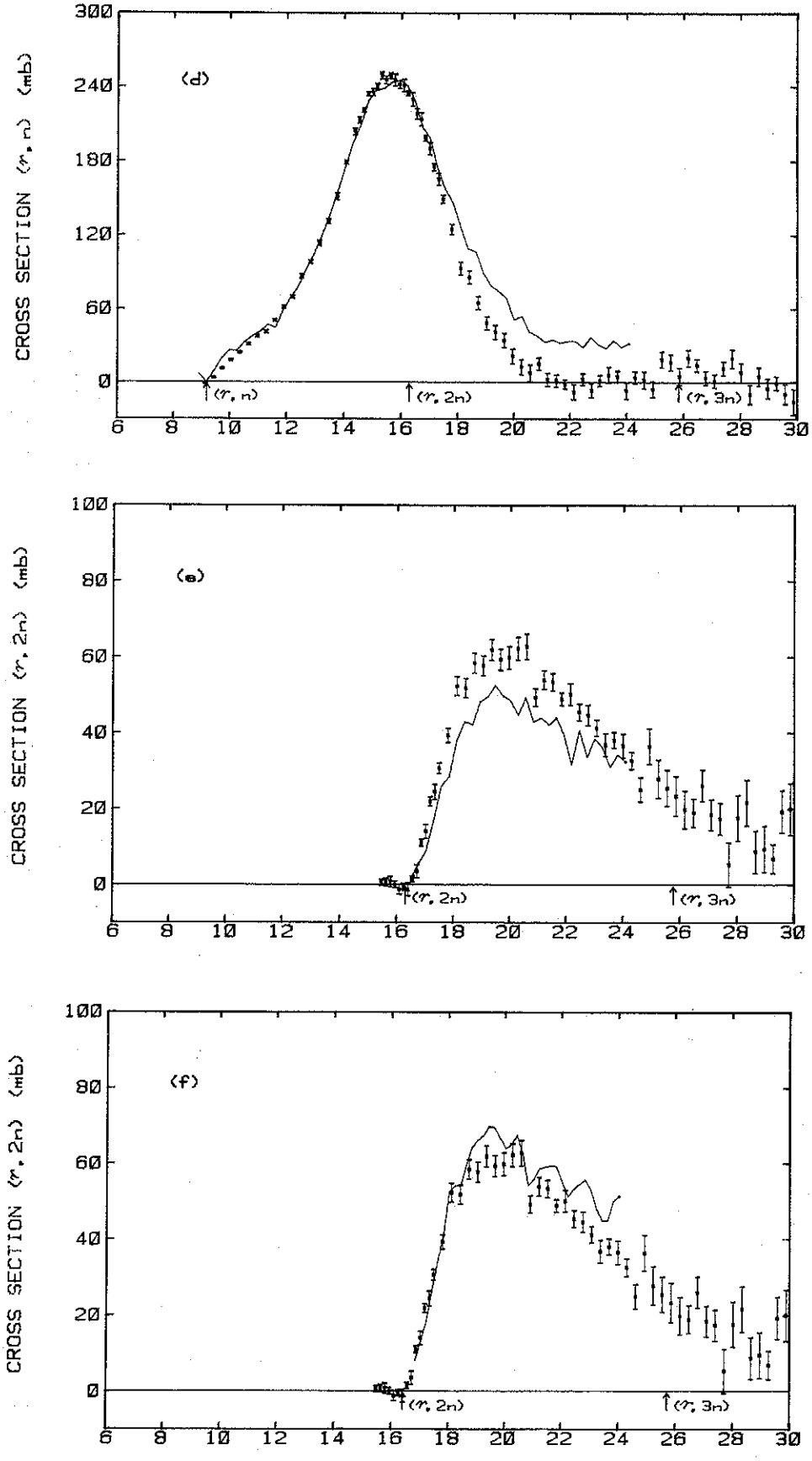
(d)
(e)
(f)
CROSS SECTION (γ, n) (mb)
CROSS SECTION (γ, 2n) (mb)
CROSS SECTION (γ, 2n) (mb)
(γ, n)
(γ, 2n)
(γ, 3n)
PHOTON ENERGY (MeV)

FIG. 7

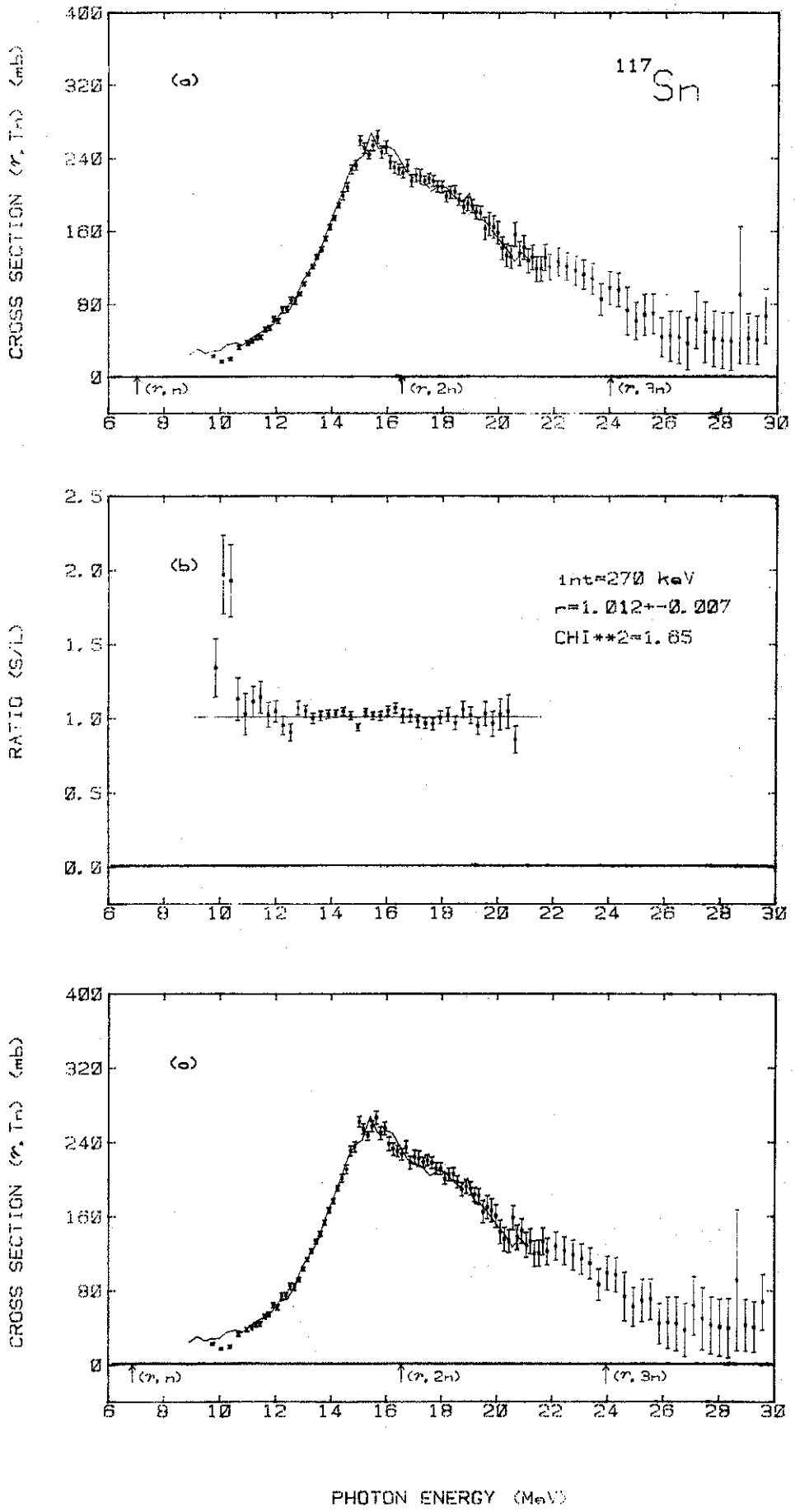
(a)
117Sn
CROSS SECTION (γ, Tn) (mb)
400
320
240
160
80
0
(γ, n)
(γ, 2n)
(γ, 3n)
6 8 10 12 14 16 18 20 22 24 26 28 30
(b)
RATIO (S/L)
2.5
2.0
1.5
1.0
0.5
0.0
int=270 keV
r=1.012+-0.007
CHI**2=1.65
(c)
CROSS SECTION (γ, Tn) (mb)
PHOTON ENERGY (MeV)

FIG. 8

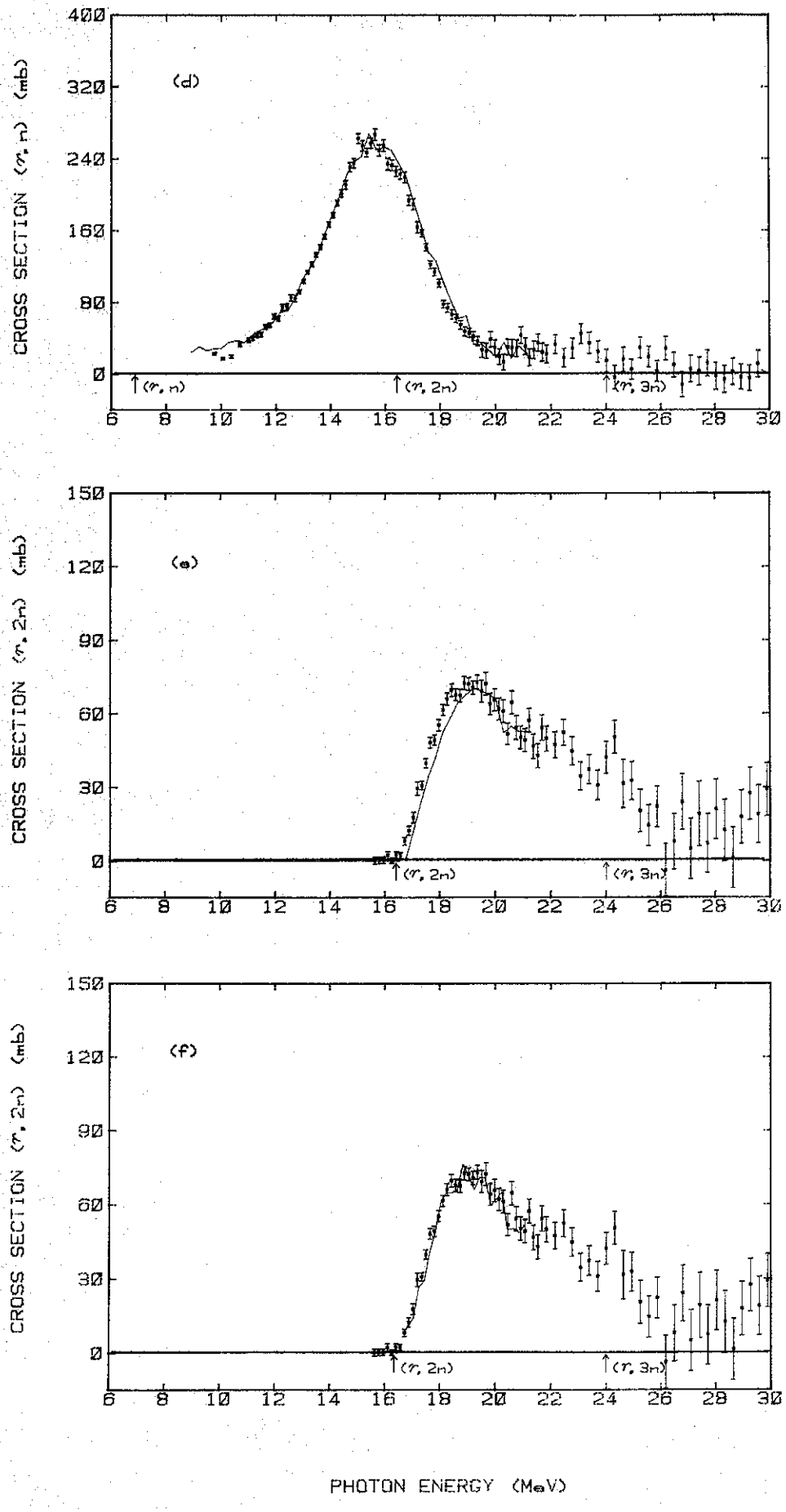
(d)
CROSS SECTION (γ, n) (mb)
400
320
240
160
80
0
(γ, n)
(γ, 2n)
(γ, 3n)
6 8 10 12 14 16 18 20 22 24 26 28 30
(e)
CROSS SECTION (γ, 2n) (mb)
150
120
90
60
30
0
(γ, 2n)
(γ, 3n)
6 8 10 12 14 16 18 20 22 24 26 28 30
(f)
CROSS SECTION (γ, 2n) (mb)
150
120
90
60
30
0
(γ, 2n)
(γ, 3n)
6 8 10 12 14 16 18 20 22 24 26 28 30
PHOTON ENERGY (MeV)

FIG. 8

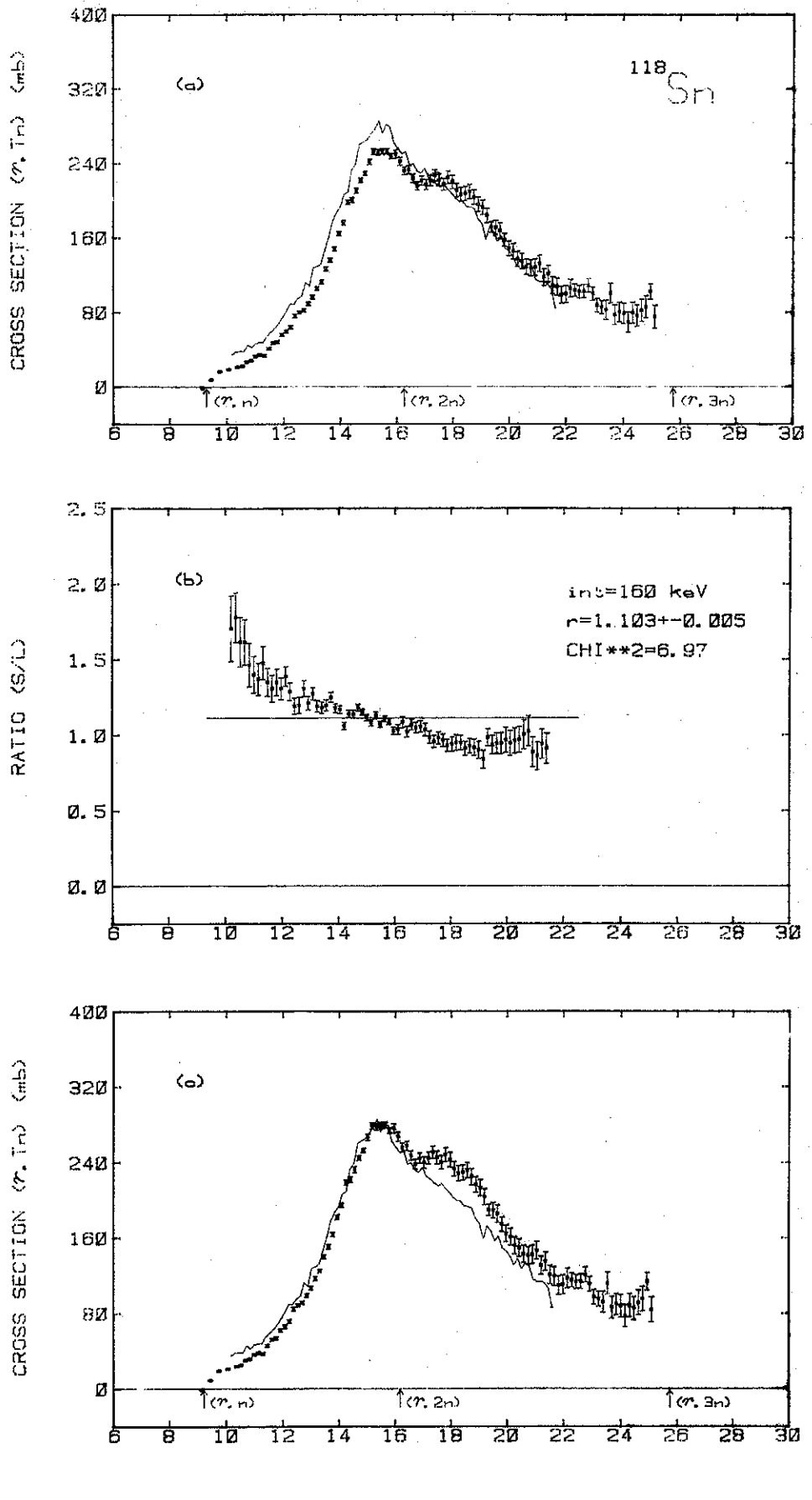
(a)
118Sn
CROSS SECTION (γ,Tn) (mb)
(γ,n)
(γ,2n)
(γ,3n)
(b)
int=160 keV
r=1.103+-0.005
CHI**2=6.97
RATIO (S/L)
(c)
CROSS SECTION (γ,Tn) (mb)
PHOTON ENERGY (MeV)

FIG. 9

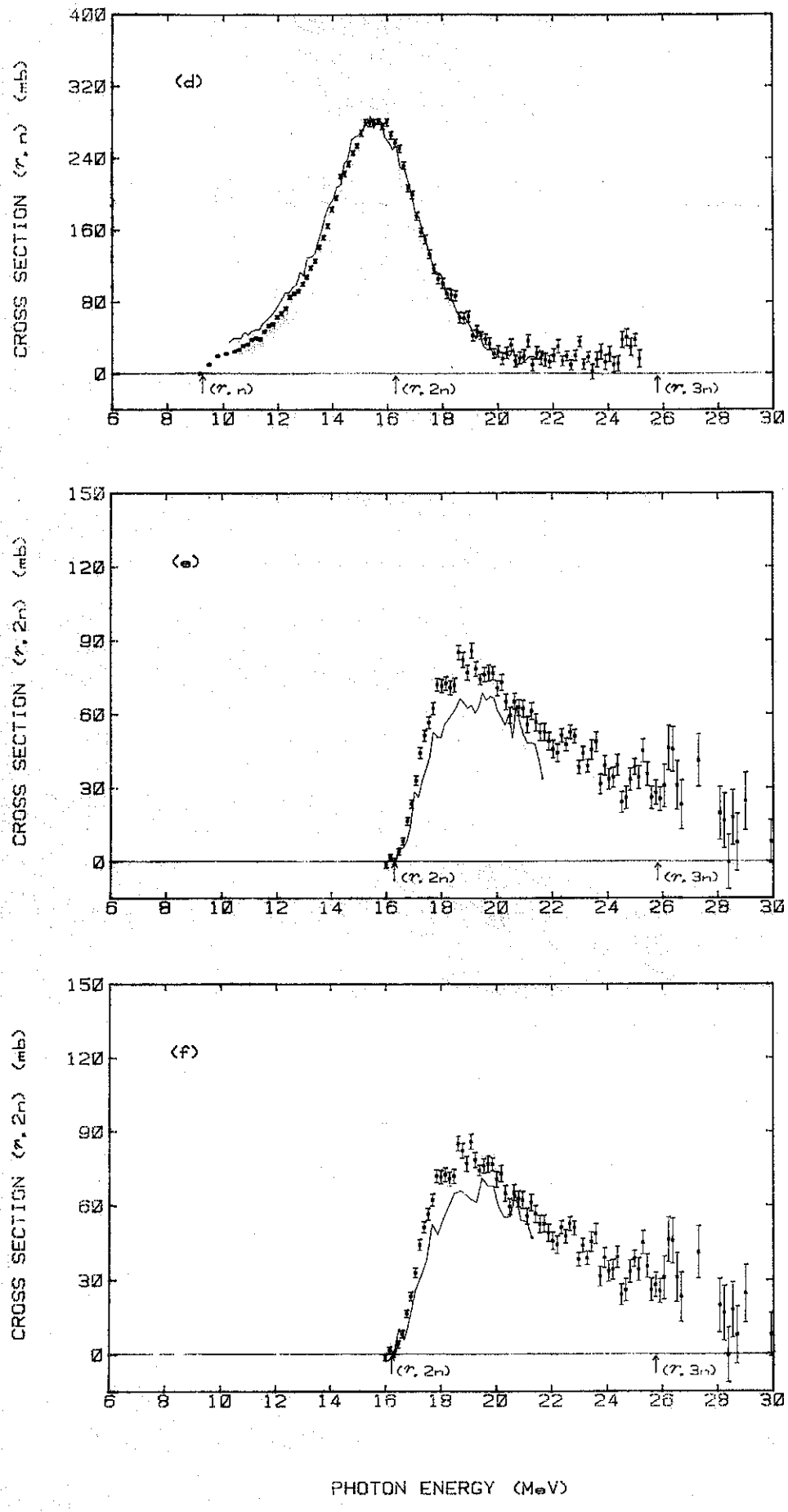
(d)
(e)
(f)
CROSS SECTION (γ, n) (mb)
CROSS SECTION (γ, 2n) (mb)
CROSS SECTION (γ, 2n) (mb)
(γ, n)
(γ, 2n)
(γ, 3n)
PHOTON ENERGY (MeV)

FIG. 9

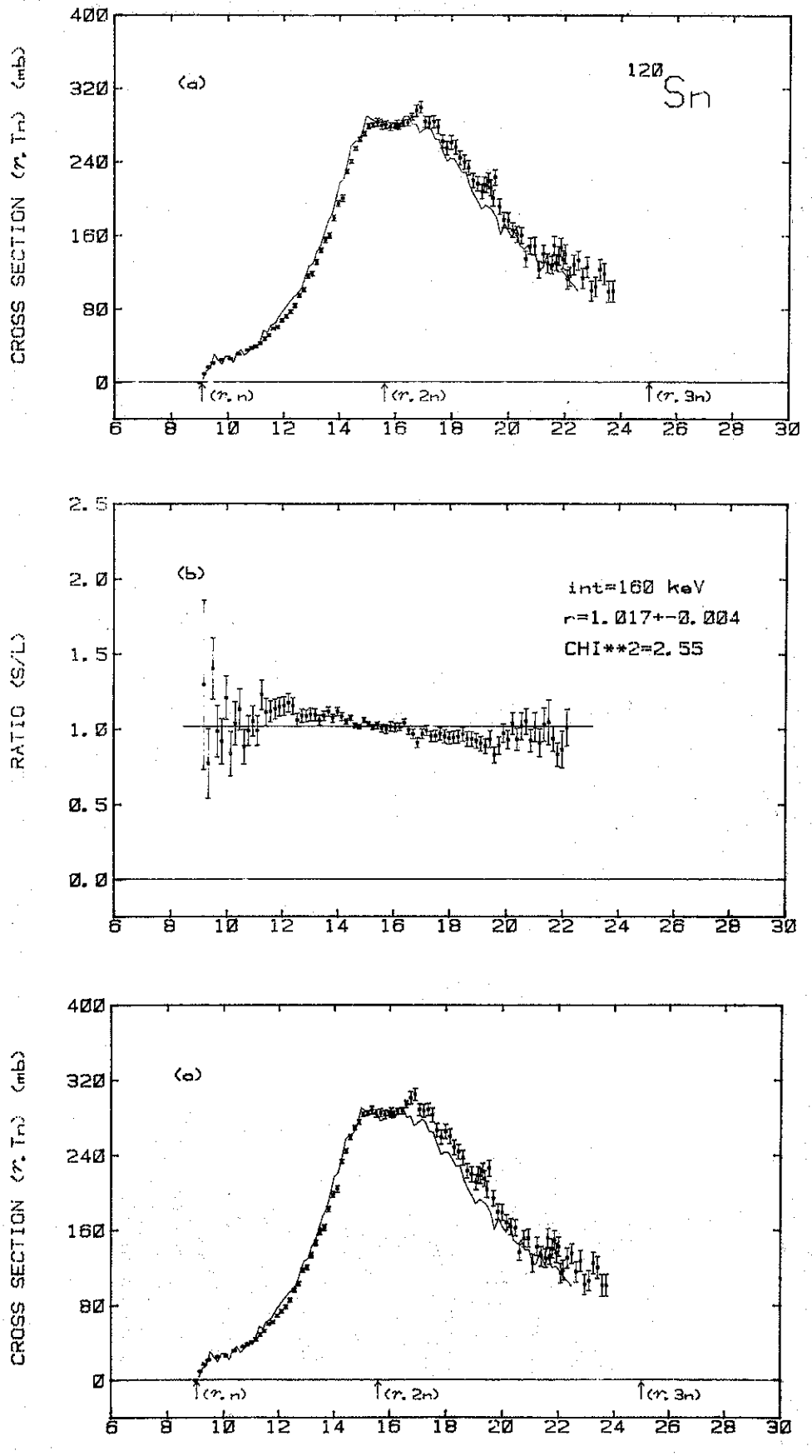
(a)
120Sn
CROSS SECTION (γ, Tn) (mb)
400
320
240
160
80
0
(γ, n)
(γ, 2n)
(γ, 3n)
6 8 10 12 14 16 18 20 22 24 26 28 30
(b)
int=160 keV
r=1.017+-0.004
CHI**2=2.55
RATIO (S/L)
2.5
2.0
1.5
1.0
0.5
0.0
6 8 10 12 14 16 18 20 22 24 26 28 30
(a)
CROSS SECTION (γ, Tn) (mb)
400
320
240
160
80
0
(γ, n)
(γ, 2n)
(γ, 3n)
6 8 10 12 14 16 18 20 22 24 26 28 30
PHOTON ENERGY (MeV)

FIG. 10

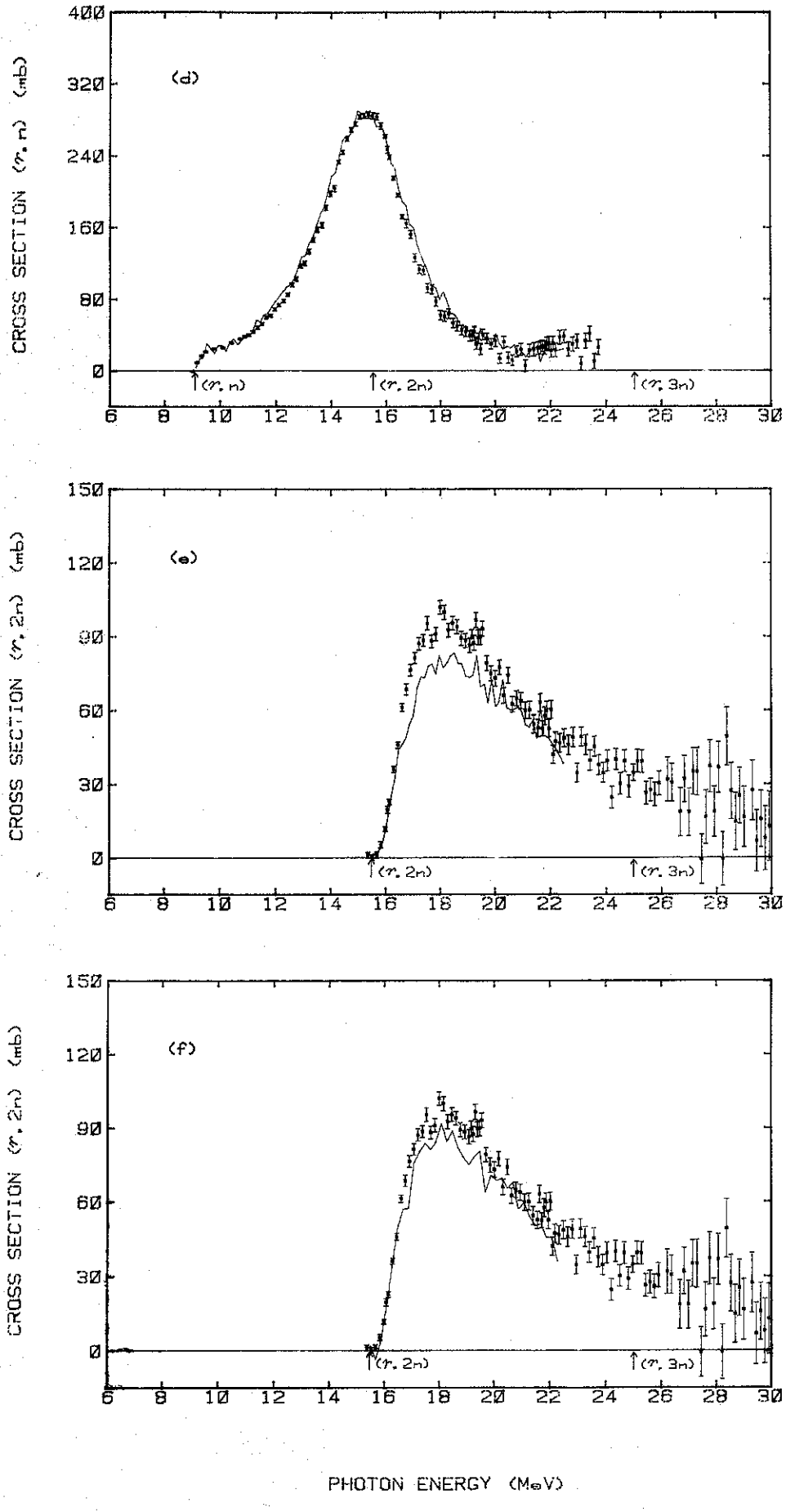
(d)
(e)
(f)
CROSS SECTION (γ, n) (mb)
CROSS SECTION (γ, 2n) (mb)
CROSS SECTION (γ, 2n) (mb)
(γ, n)
(γ, 2n)
(γ, 3n)
PHOTON ENERGY (MeV)

FIG. 10

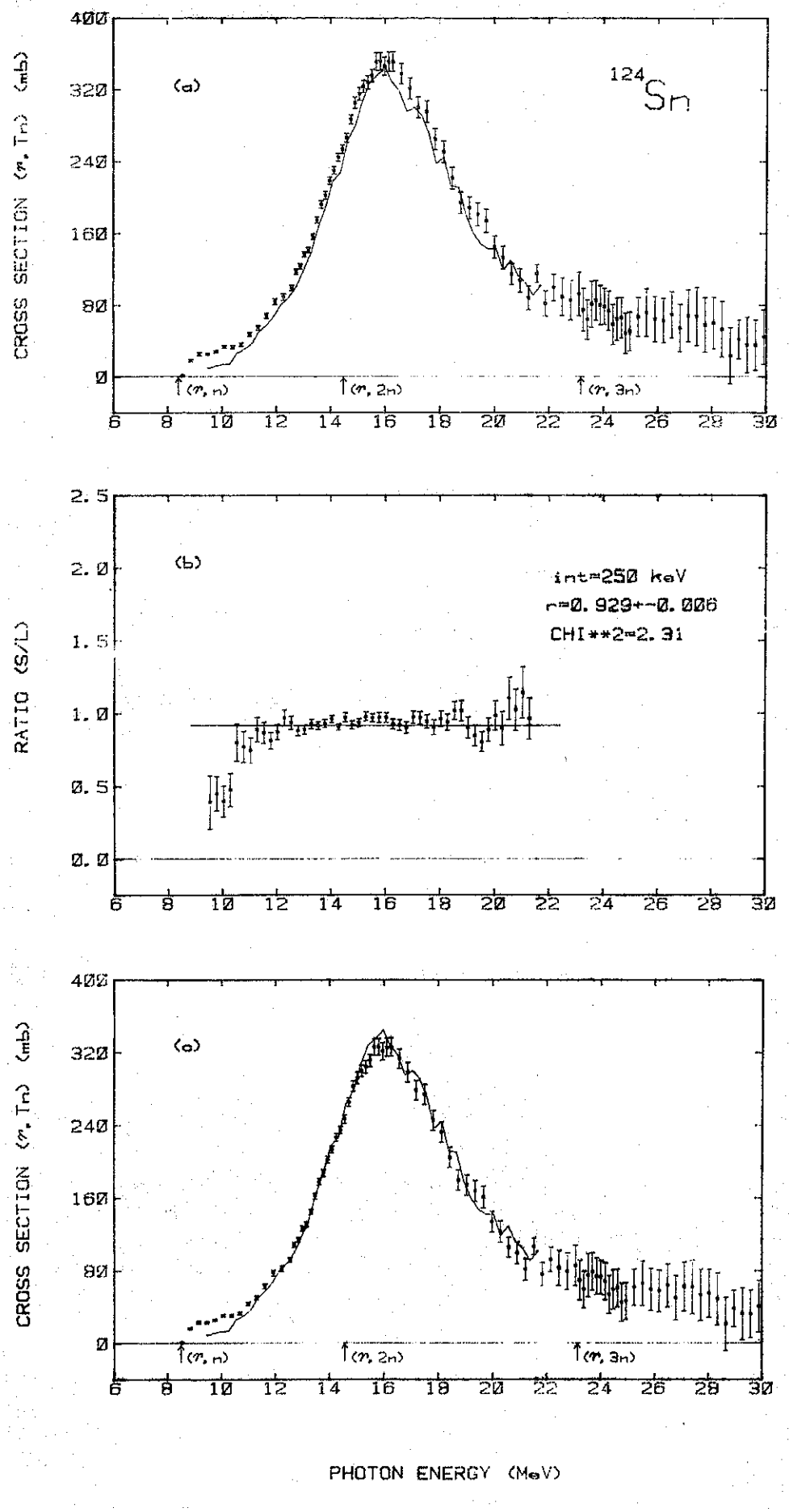
CROSS SECTION (γ, Tn) (mb)
400
320
240
160
80
0
(a)
124Sn
(γ, n)
(γ, 2n)
(γ, 3n)
6 8 10 12 14 16 18 20 22 24 26 28 30
RATIO (S/L)
2.5
2.0
1.5
1.0
0.5
0.0
(b)
int=250 keV
r=0.929+-0.006
CHI**2=2.31
CROSS SECTION (γ, Tn) (mb)
400
320
240
160
80
0
(a)
(γ, n)
(γ, 2n)
(γ, 3n)
6 8 10 12 14 16 18 20 22 24 26 28 30
PHOTON ENERGY (MeV)

FIG. 11

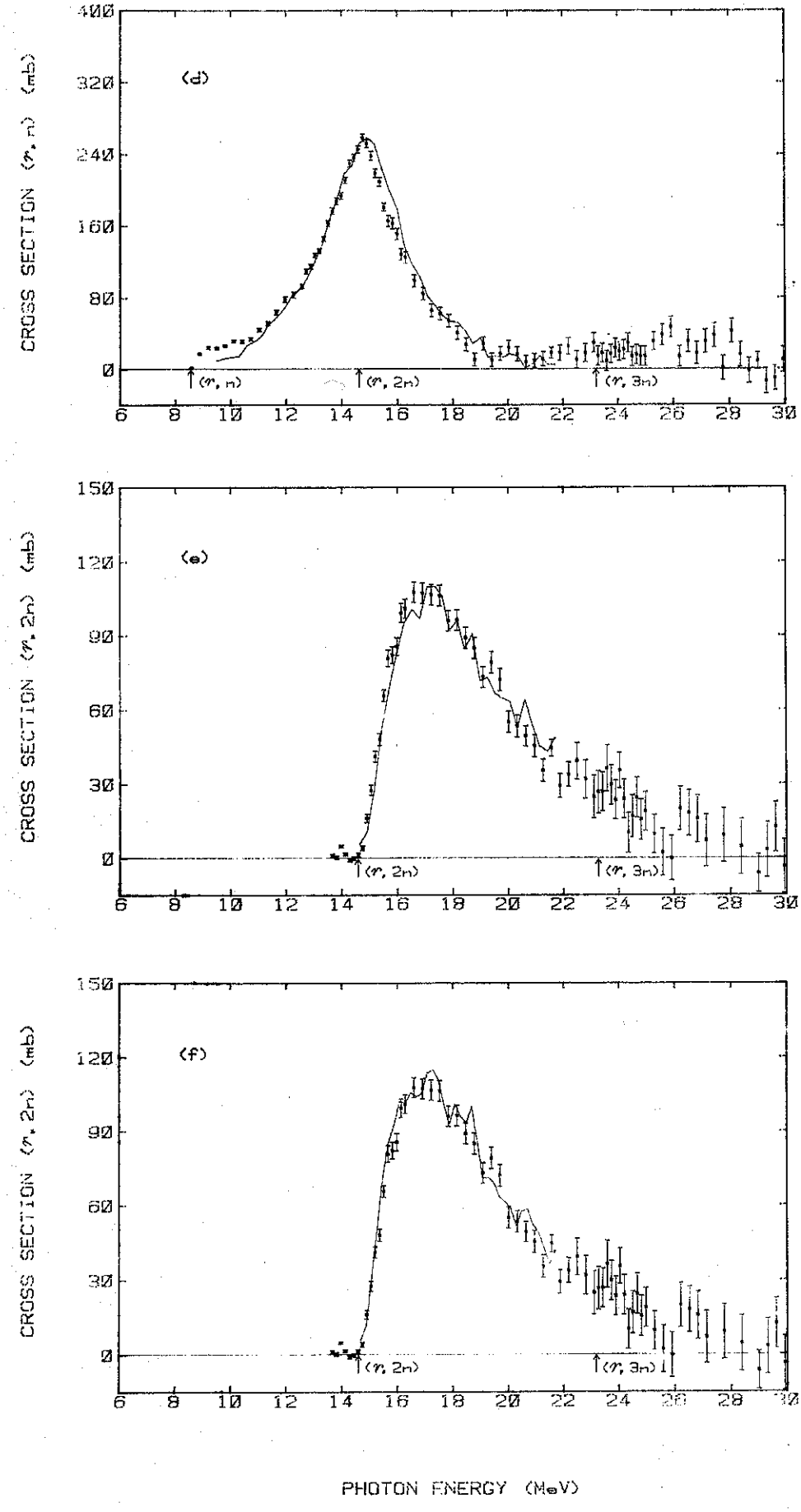
(d)
(e)
(f)
CROSS SECTION (γ, n) (mb)
CROSS SECTION (γ, 2n) (mb)
CROSS SECTION (γ, 2n) (mb)
(γ, n)
(γ, 2n)
(γ, 3n)
PHOTON ENERGY (MeV)

FIG. 11

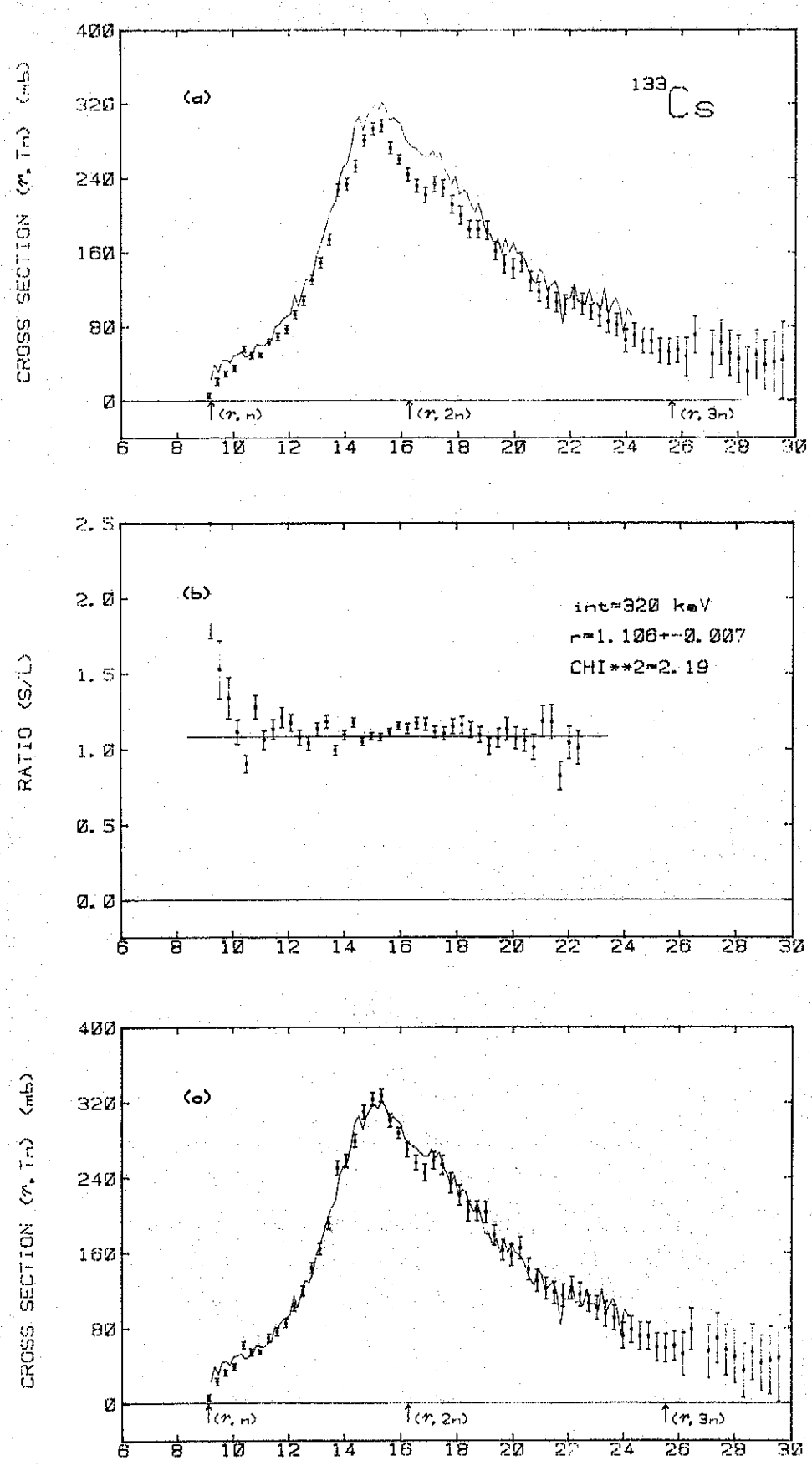
(a)
133Cs
CROSS SECTION (γ, Tn) (mb)
400
320
240
160
80
0
(γ, n)
(γ, 2n)
(γ, 3n)
6 8 10 12 14 16 18 20 22 24 26 28 30
(b)
int=320 keV
r=1.106+-0.007
CHI**2=2.19
RATIO (S/L)
2.5
2.0
1.5
1.0
0.5
0.0
(c)
CROSS SECTION (γ, Tn) (mb)
PHOTON ENERGY (MeV)

FIG. 12

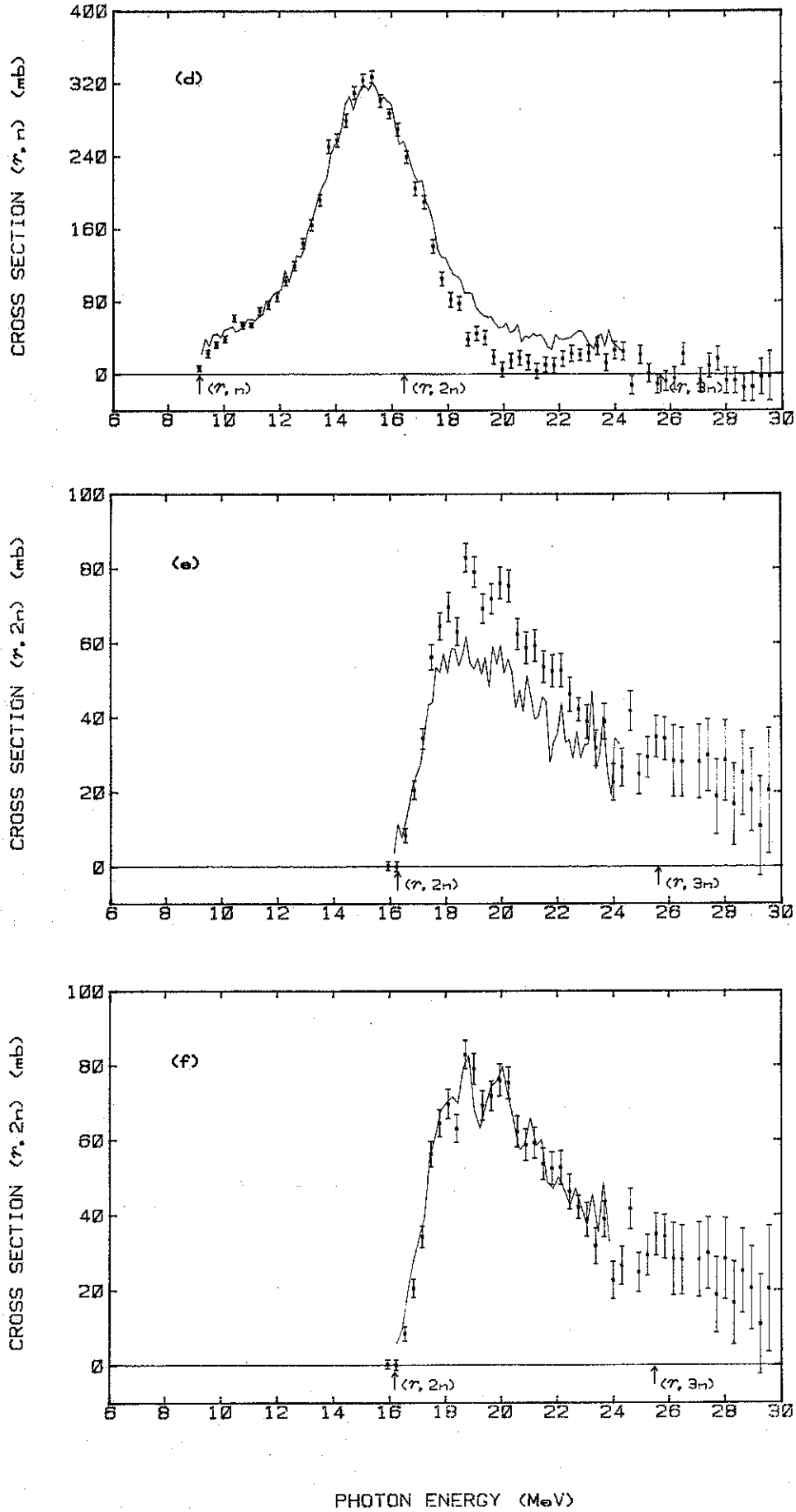
(d)
CROSS SECTION (γ, n) (mb)
400
320
240
160
80
0
(γ, n)
(γ, 2n)
(γ, 3n)
6 8 10 12 14 16 18 20 22 24 26 28 30
(e)
CROSS SECTION (γ, 2n) (mb)
100
80
60
40
20
0
(γ, 2n)
(γ, 3n)
6 8 10 12 14 16 18 20 22 24 26 28 30
(f)
CROSS SECTION (γ, 2n) (mb)
100
80
60
40
20
0
(γ, 2n)
(γ, 3n)
6 8 10 12 14 16 18 20 22 24 26 28 30
PHOTON ENERGY (MeV)

FIG. 12

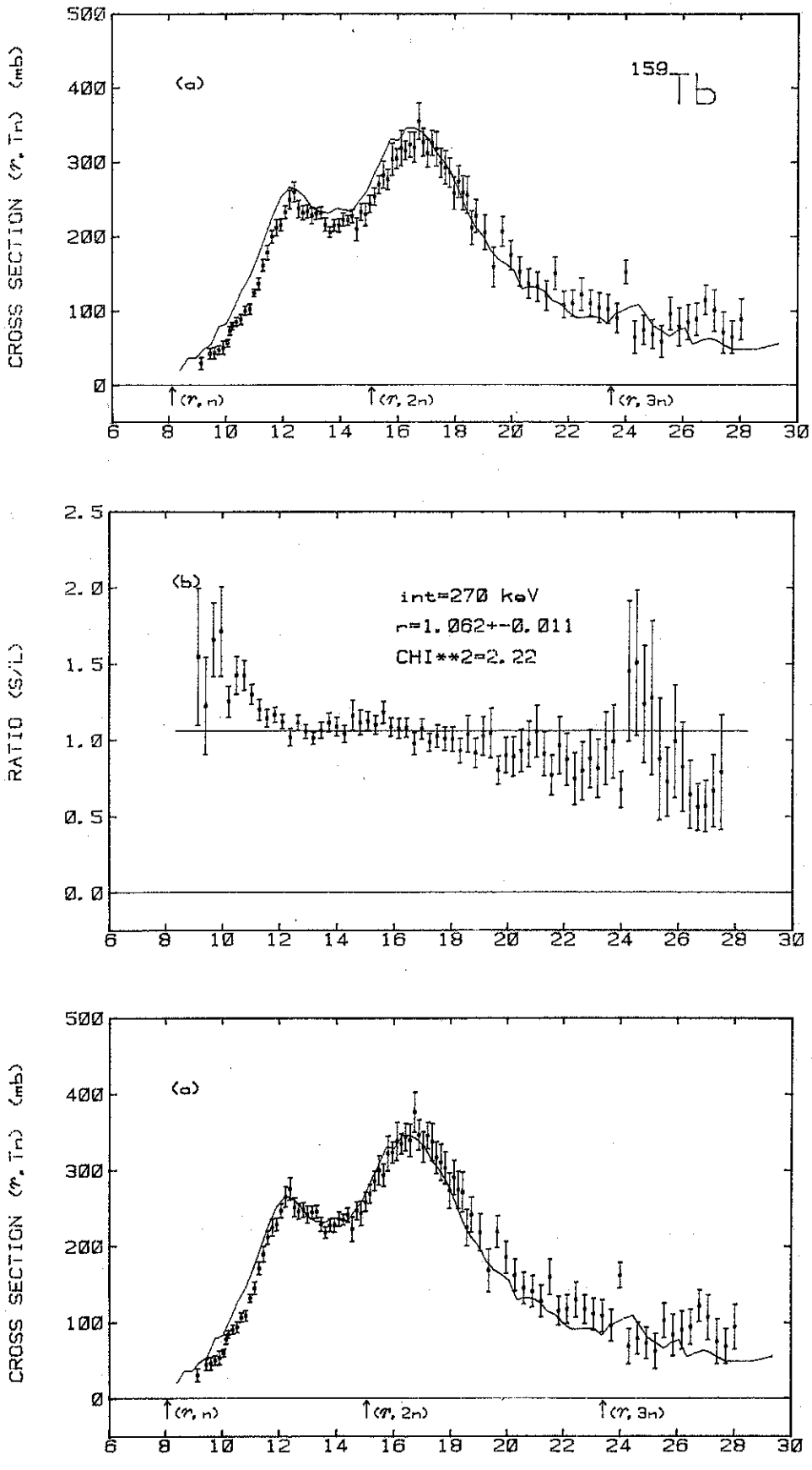
CROSS SECTION (γ, Tn) (mb)
(a)
159Tb
(γ, n)
(γ, 2n)
(γ, 3n)
RATIO (S/L)
(b)
int=270 keV
r=1.062+-0.011
CHI**2=2.22
CROSS SECTION (γ, Tn) (mb)
(a)
PHOTON ENERGY (MeV)

FIG. 13

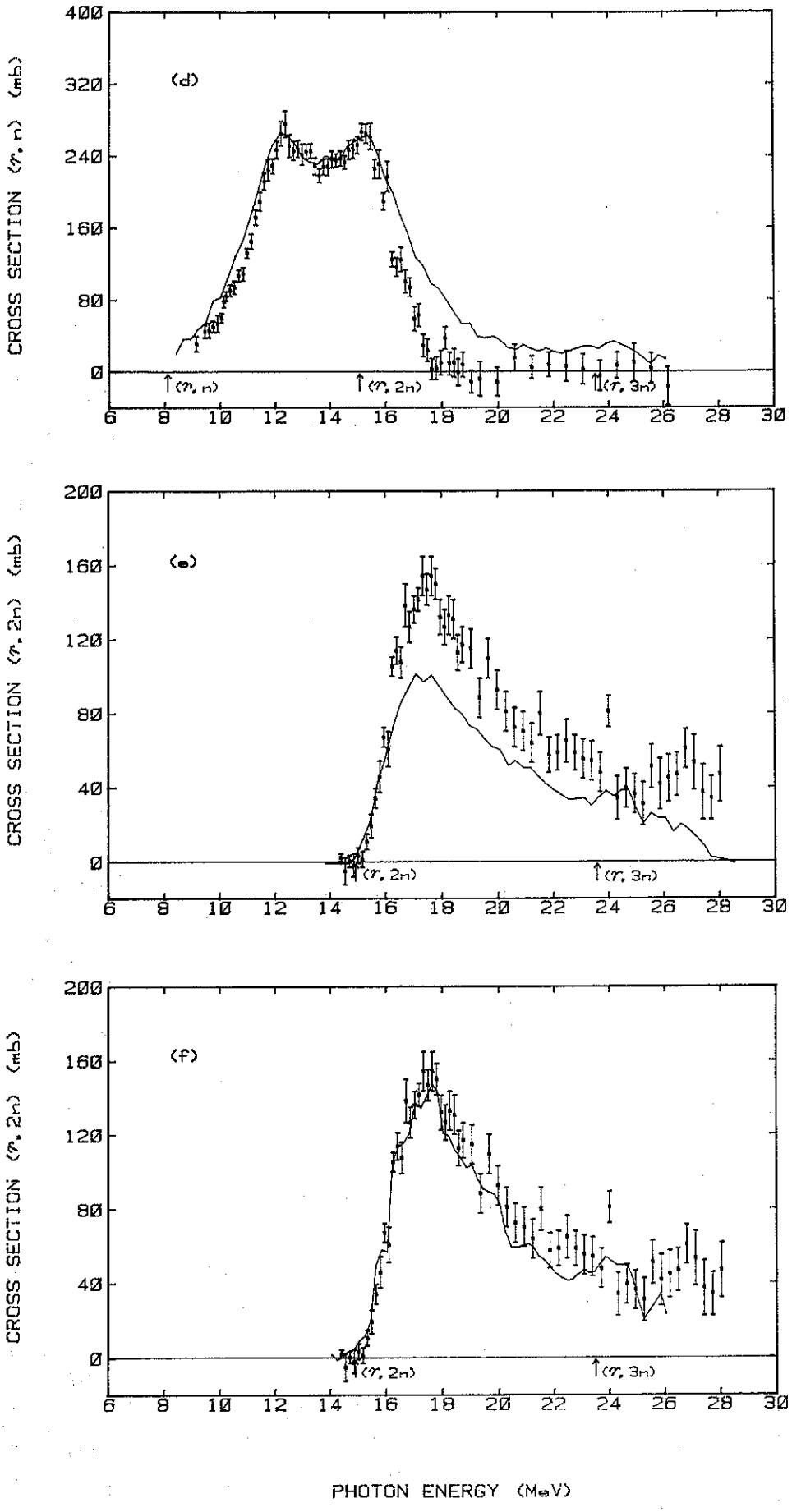
CROSS SECTION (γ, n) (mb)
(d)
(γ, n)
(γ, 2n)
(γ, 3n)
CROSS SECTION (γ, 2n) (mb)
(e)
(γ, 2n)
(γ, 3n)
CROSS SECTION (γ, 2n) (mb)
(f)
(γ, 2n)
(γ, 3n)
PHOTON ENERGY (MeV)

FIG. 13

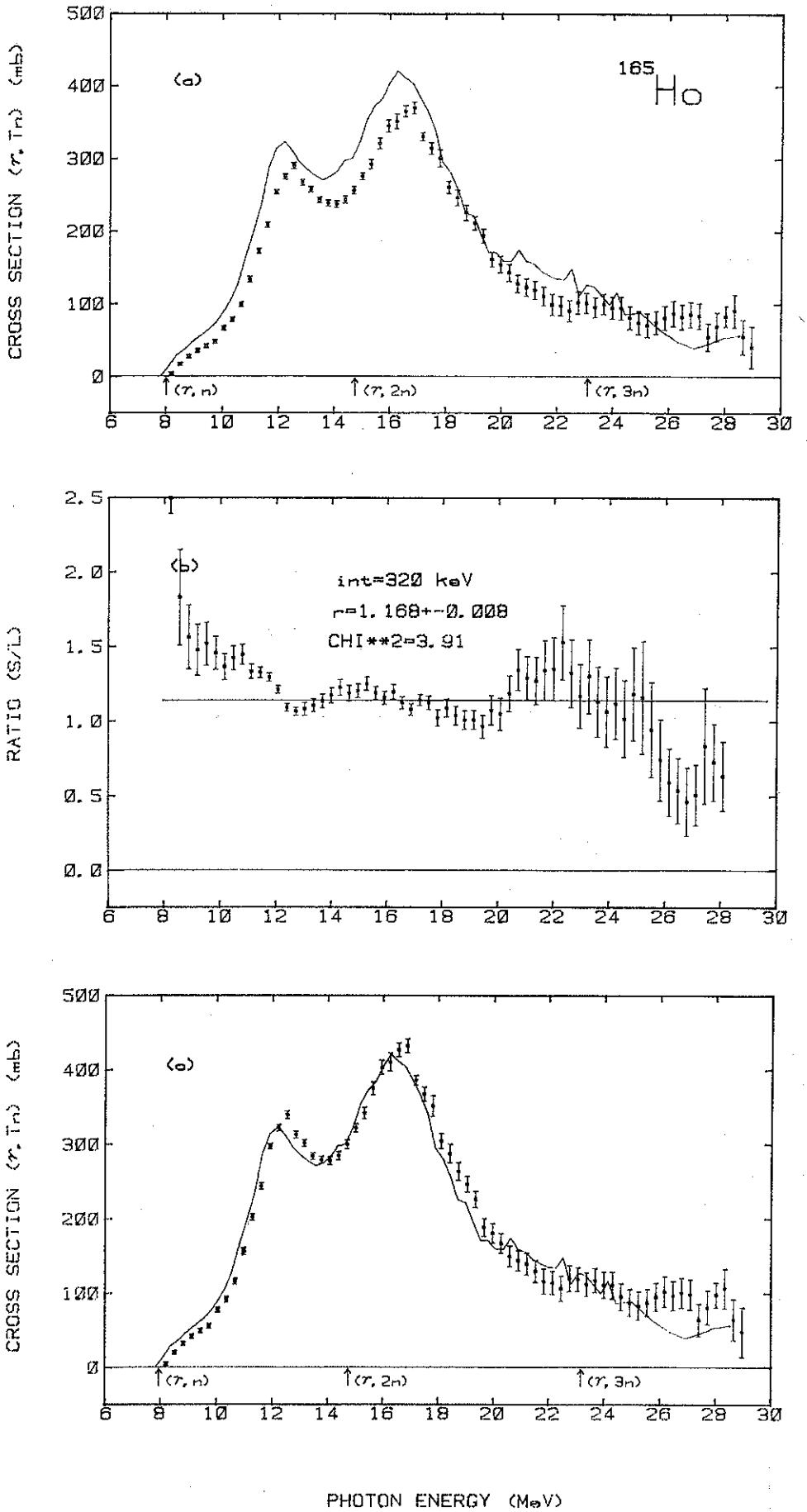
(a)
165Ho
CROSS SECTION (γ, Tn) (mb)
(γ, n)
(γ, 2n)
(γ, 3n)
(b)
int=320 keV
r=1.168+-0.008
CHI**2=3.91
RATIO (S/L)
PHOTON ENERGY (MeV)

FIG. 14

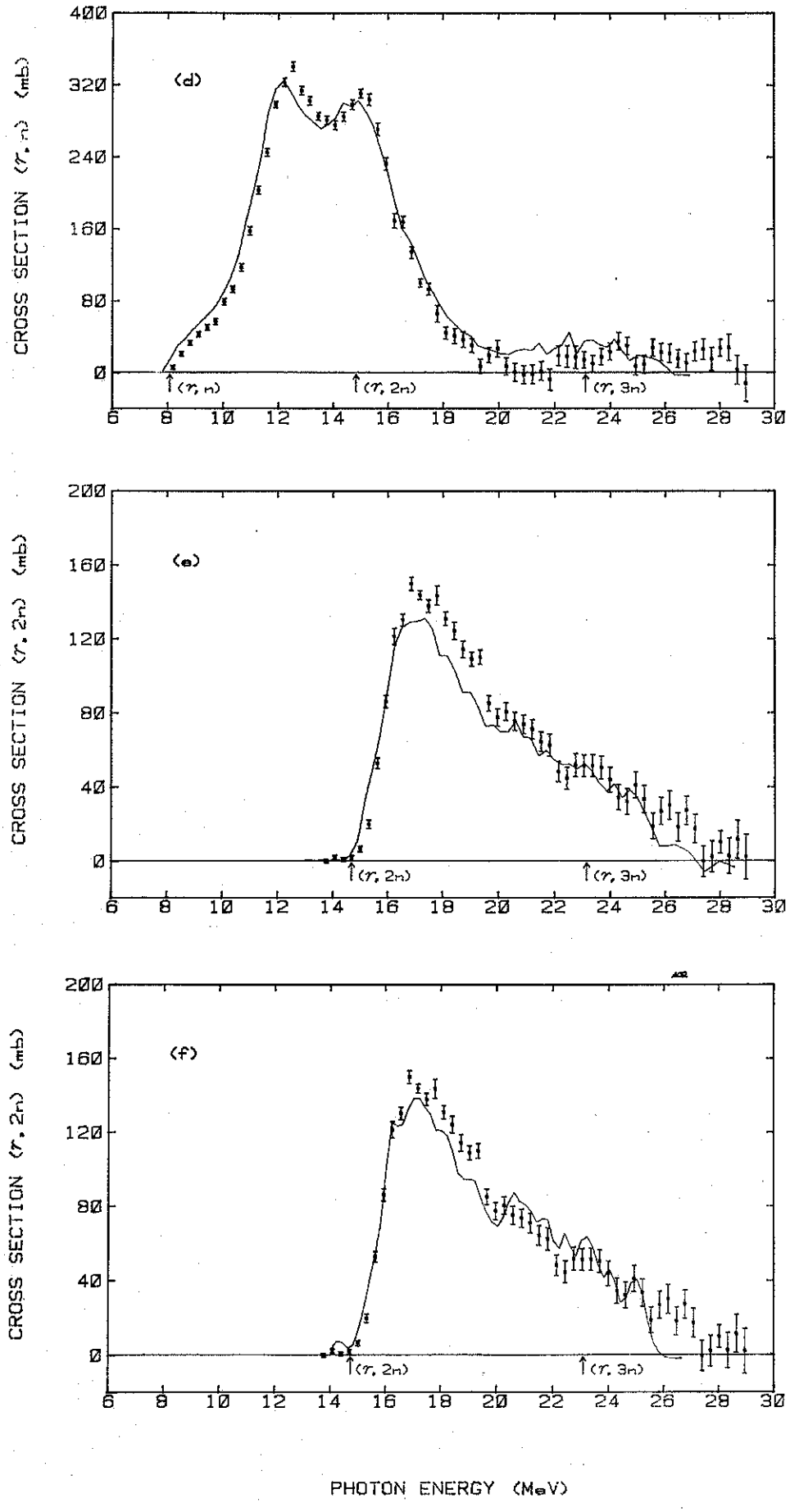
(d)
CROSS SECTION (γ, n) (mb)
400
320
240
160
80
0
(γ, n)
(γ, 2n)
(γ, 3n)
6 8 10 12 14 16 18 20 22 24 26 28 30
(e)
CROSS SECTION (γ, 2n) (mb)
200
160
120
80
40
0
(γ, 2n)
(γ, 3n)
6 8 10 12 14 16 18 20 22 24 26 28 30
(f)
CROSS SECTION (γ, 2n) (mb)
200
160
120
80
40
0
(γ, 2n)
(γ, 3n)
6 8 10 12 14 16 18 20 22 24 26 28 30
PHOTON ENERGY (MeV)

FIG. 14

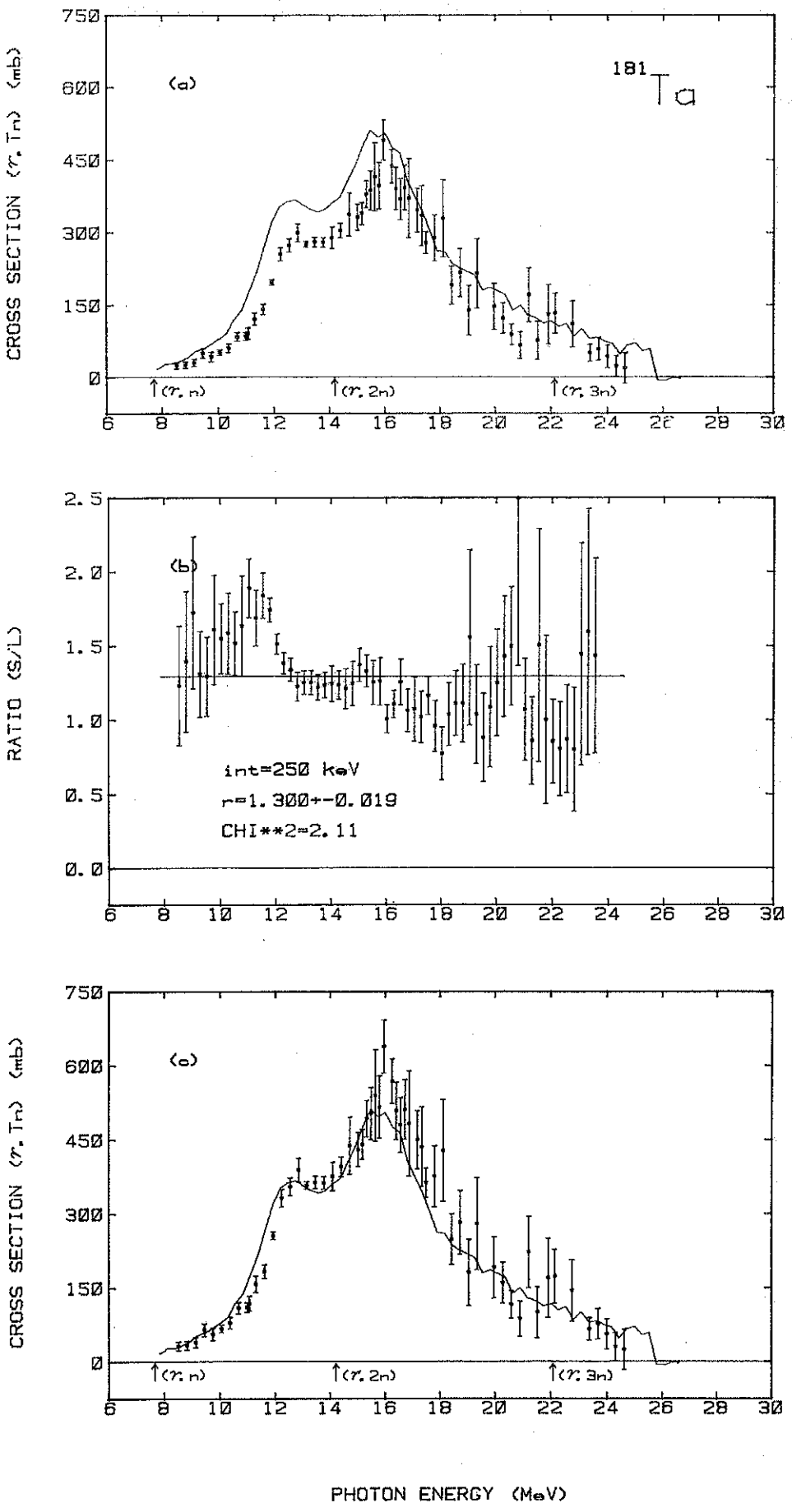
CROSS SECTION (γ, Tn) (mb)
(a)
181 Ta
750
600
450
300
150
0
(γ, n)
(γ, 2n)
(γ, 3n)
6 8 10 12 14 16 18 20 22 24 26 28 30
RATIO (S/L)
(b)
2.5
2.0
1.5
1.0
0.5
0.0
int=250 keV
r=1.300+-0.019
CHI**2=2.11
(c)
PHOTON ENERGY (MeV)

FIG. 15

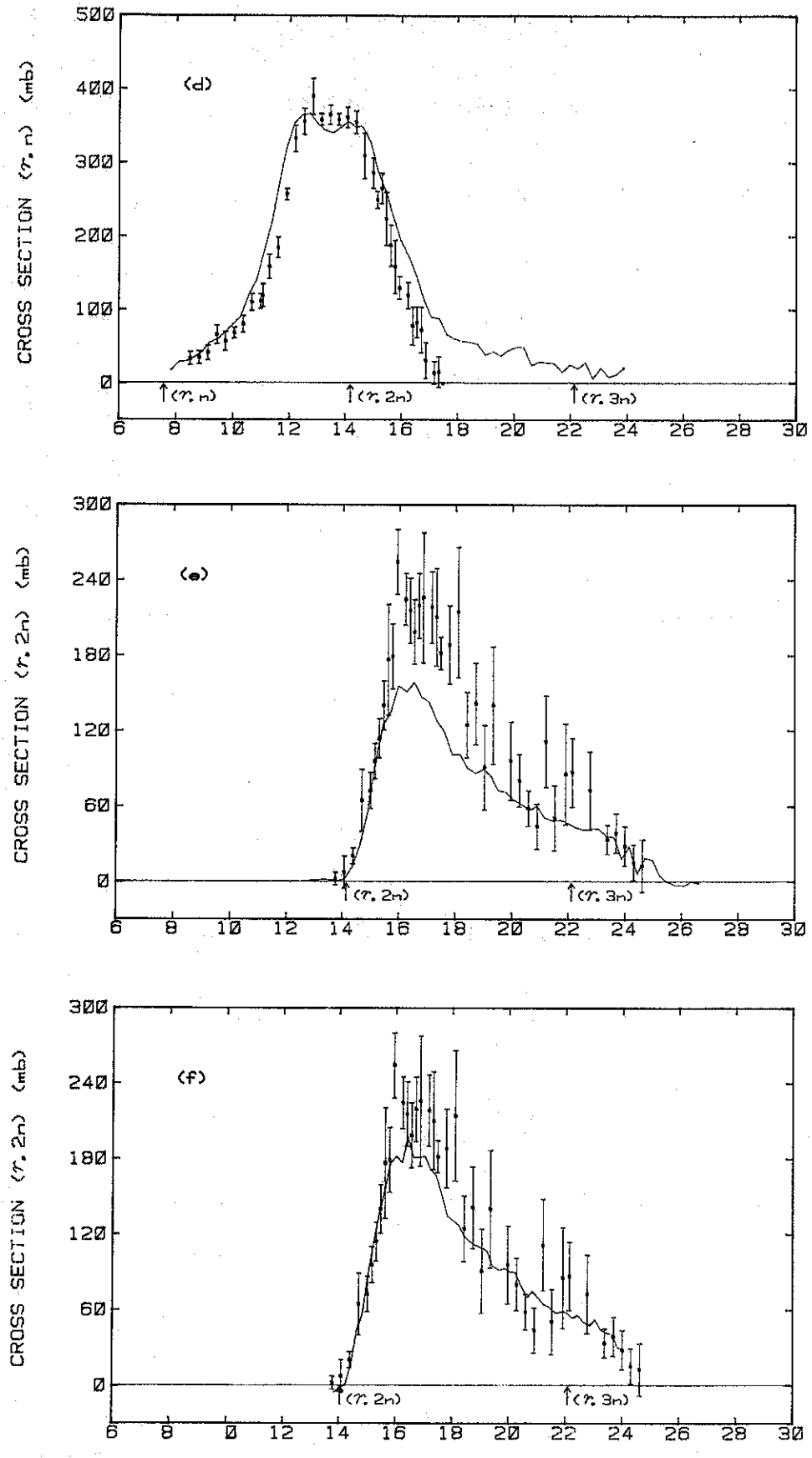
(d)
CROSS SECTION (γ, n) (mb)
500
400
300
200
100
0
(γ, n)
(γ, 2n)
(γ, 3n)
6 8 10 12 14 16 18 20 22 24 26 28 30
(e)
CROSS SECTION (γ, 2n) (mb)
300
240
180
120
60
0
(γ, 2n)
(γ, 3n)
6 8 10 12 14 16 18 20 22 24 26 28 30
(f)
CROSS SECTION (γ, 2n) (mb)
300
240
180
120
60
0
(γ, 2n)
(γ, 3n)
6 8 0 12 14 16 18 20 22 24 26 28 30
PHOTON ENERGY (MeV)

FIG. 15

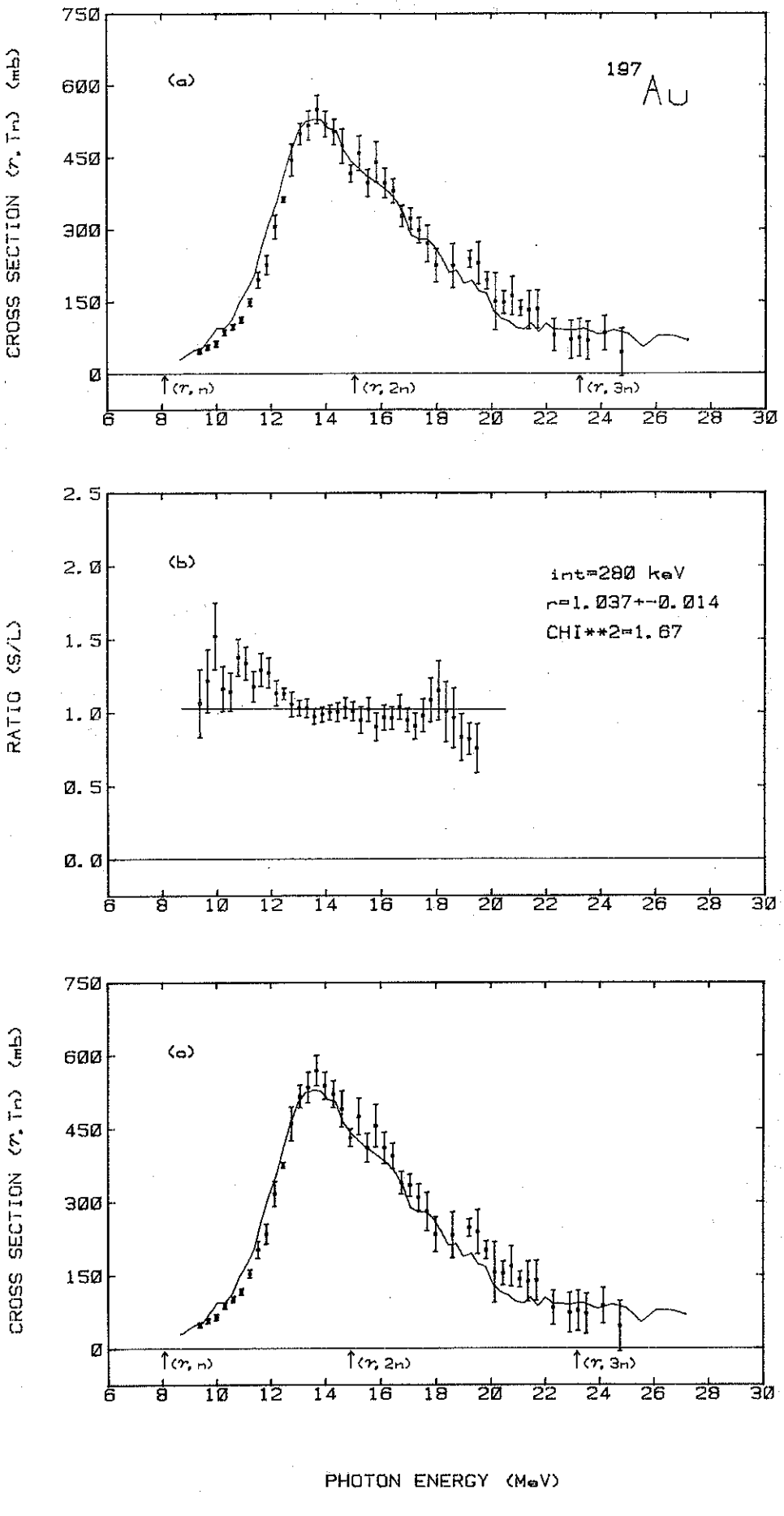
(a)
197 Au
CROSS SECTION (γ, Tn) (mb)
(γ, n)
(γ, 2n)
(γ, 3n)
(b)
int=280 keV
r=1.037+-0.014
CHI**2=1.67
RATIO (S/L)
PHOTON ENERGY (MeV)

FIG. 16

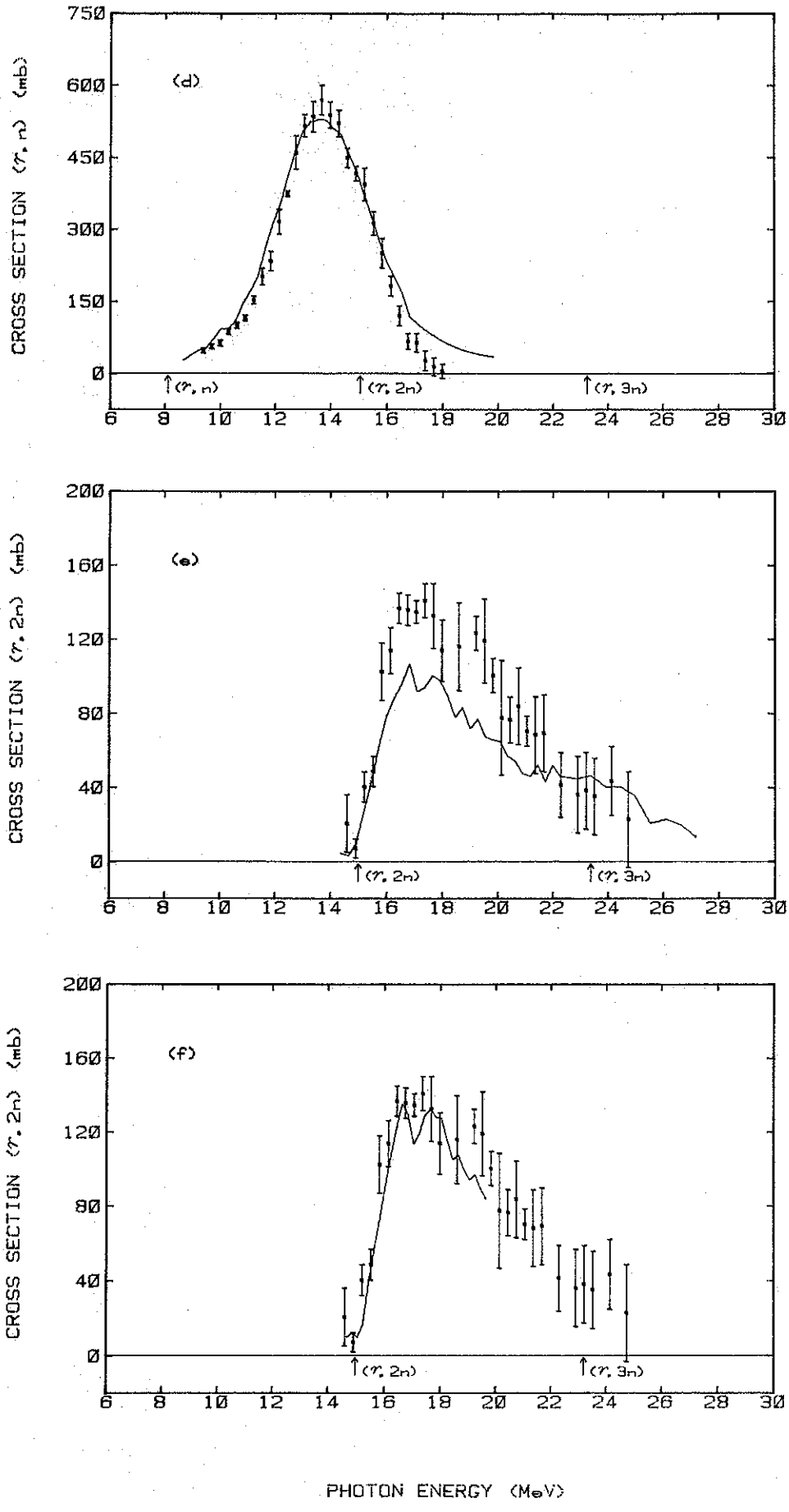
(d)
CROSS SECTION (γ, n) (mb)
750
600
450
300
150
0
(γ, n)
(γ, 2n)
(γ, 3n)
6 8 10 12 14 16 18 20 22 24 26 28 30
(e)
CROSS SECTION (γ, 2n) (mb)
200
160
120
80
40
0
(γ, 2n)
(γ, 3n)
6 8 10 12 14 16 18 20 22 24 26 28 30
(f)
CROSS SECTION (γ, 2n) (mb)
200
160
120
80
40
0
(γ, 2n)
(γ, 3n)
6 8 10 12 14 16 18 20 22 24 26 28 30
PHOTON ENERGY (MeV)

FIG. 16

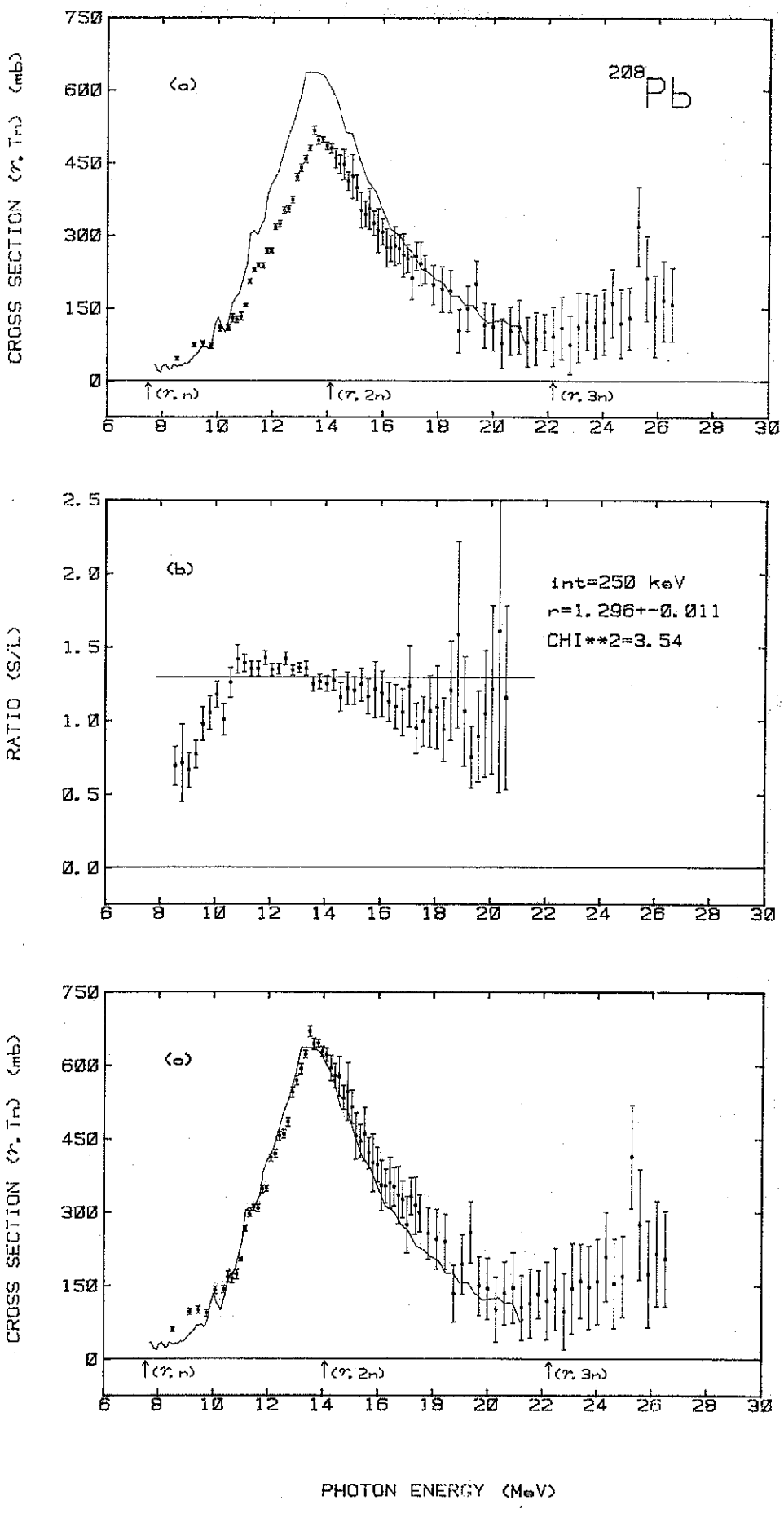
CROSS SECTION (γ, Tn) (mb)
750
600
450
300
150
0
(a)
208Pb
↑(γ, n)
↑(γ, 2n)
↑(γ, 3n)
6 8 10 12 14 16 18 20 22 24 26 28 30
RATIO (S/L)
2.5
2.0
1.5
1.0
0.5
0.0
(b)
int=250 keV
r=1.296+-0.011
CHI**2=3.54
CROSS SECTION (γ, Tn) (mb)
PHOTON ENERGY (MeV)

FIG. 17

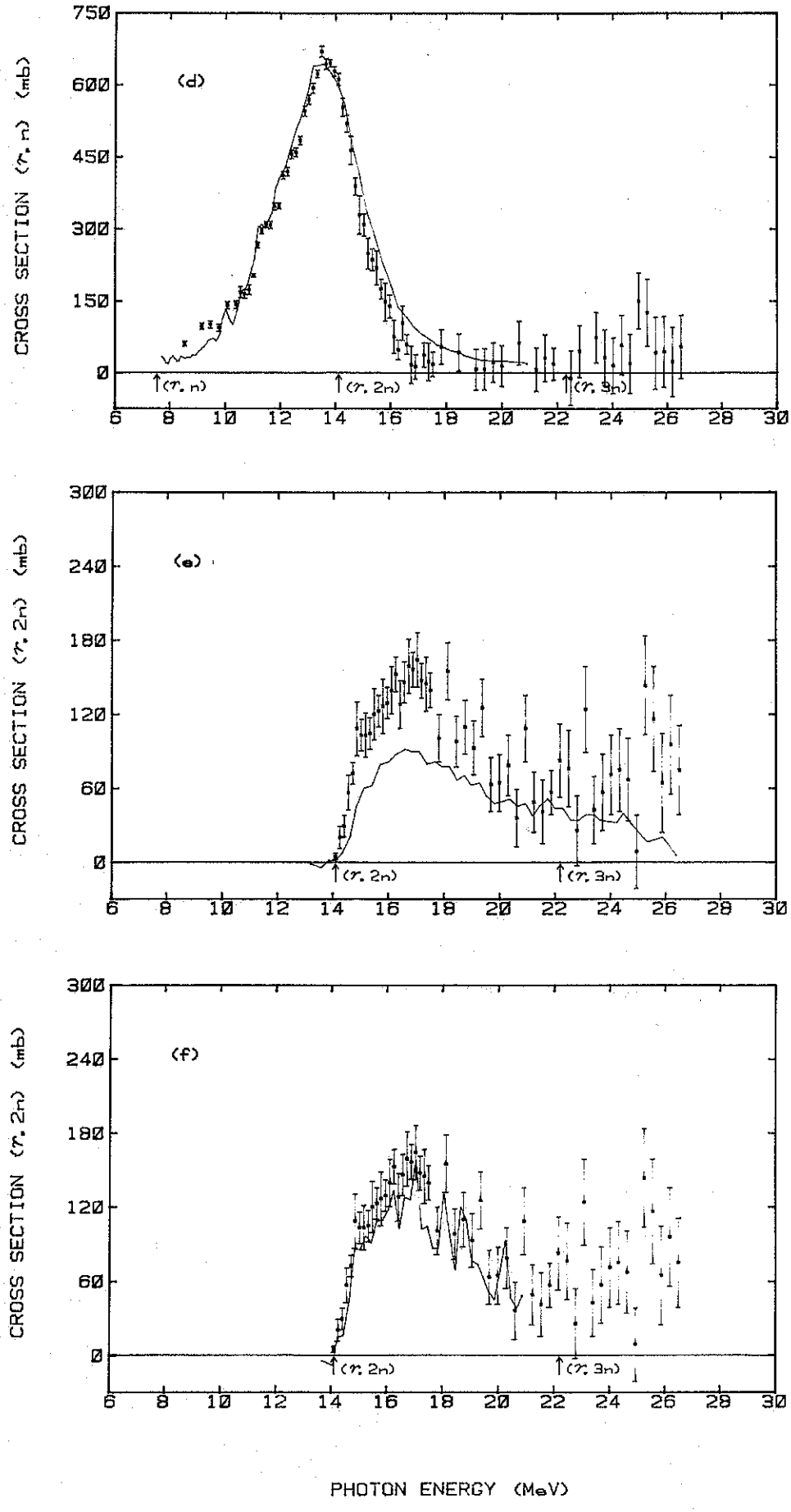
(d)
CROSS SECTION (γ, n) (mb)
750
600
450
300
150
0
(γ, n)
(γ, 2n)
(γ, 3n)
6 8 10 12 14 16 18 20 22 24 26 28 30
(e)
CROSS SECTION (γ, 2n) (mb)
300
240
180
120
60
0
(γ, 2n)
(γ, 3n)
6 8 10 12 14 16 18 20 22 24 26 28 30
(f)
CROSS SECTION (γ, 2n) (mb)
300
240
180
120
60
0
(γ, 2n)
(γ, 3n)
6 8 10 12 14 16 18 20 22 24 26 28 30
PHOTON ENERGY (MeV)

FIG. 17

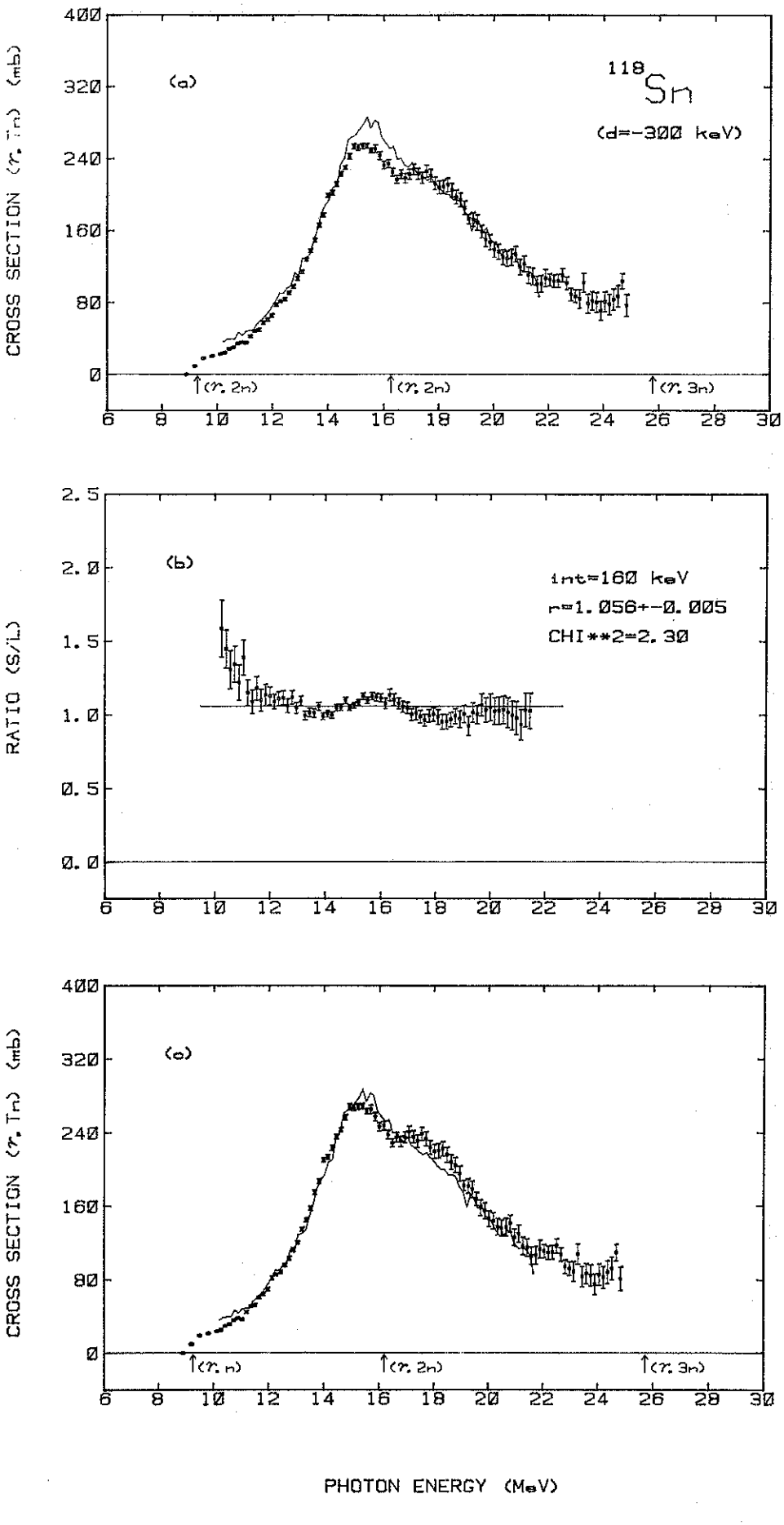
(a)
118Sn
(d=-300 keV)
CROSS SECTION (γ,Tn) (mb)
400
320
240
160
80
0
(γ,2n)
(γ,2n)
(γ,3n)
6 8 10 12 14 16 18 20 22 24 26 28 30
(b)
int=160 keV
r=1.056+-0.005
CHI**2=2.30
RATIO (S/L)
2.5
2.0
1.5
1.0
0.5
0.0
6 8 10 12 14 16 18 20 22 24 26 28 30
(c)
CROSS SECTION (γ,Tn) (mb)
400
320
240
160
80
0
(γ,n)
(γ,2n)
(γ,3n)
6 8 10 12 14 16 18 20 22 24 26 28 30
PHOTON ENERGY (MeV)

FIG. 18

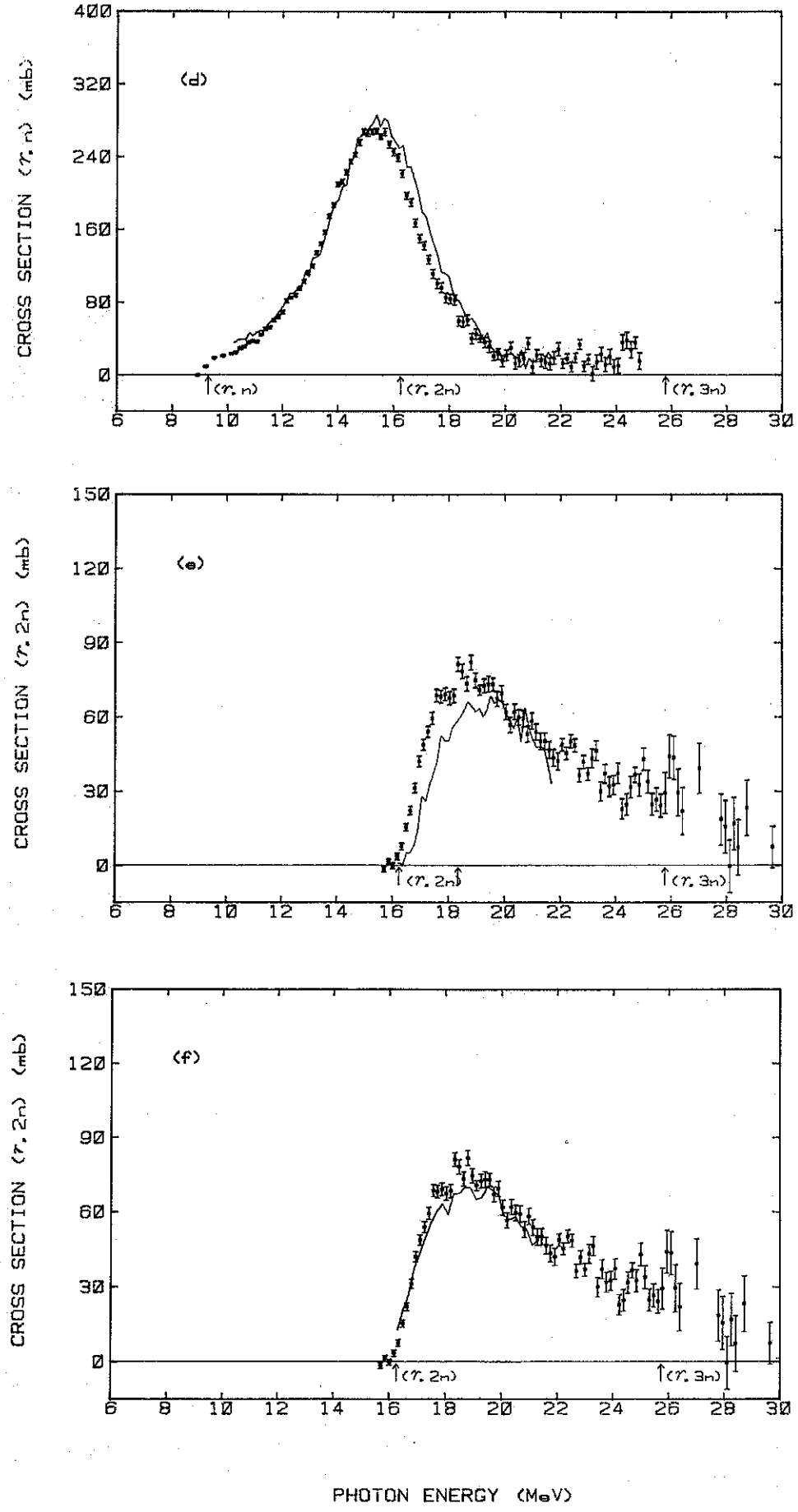
(d)
CROSS SECTION (γ, n) (mb)
400
320
240
160
80
0
(γ, n)
(γ, 2n)
(γ, 3n)
6 8 10 12 14 16 18 20 22 24 26 28 30
(e)
CROSS SECTION (γ, 2n) (mb)
150
120
90
60
30
0
(γ, 2n)
(γ, 3n)
6 8 10 12 14 16 18 20 22 24 26 28 30
(f)
CROSS SECTION (γ, 2n) (mb)
150
120
90
60
30
0
(γ, 2n)
(γ, 3n)
6 8 10 12 14 16 18 20 22 24 26 28 30
PHOTON ENERGY (MeV)

FIG. 18

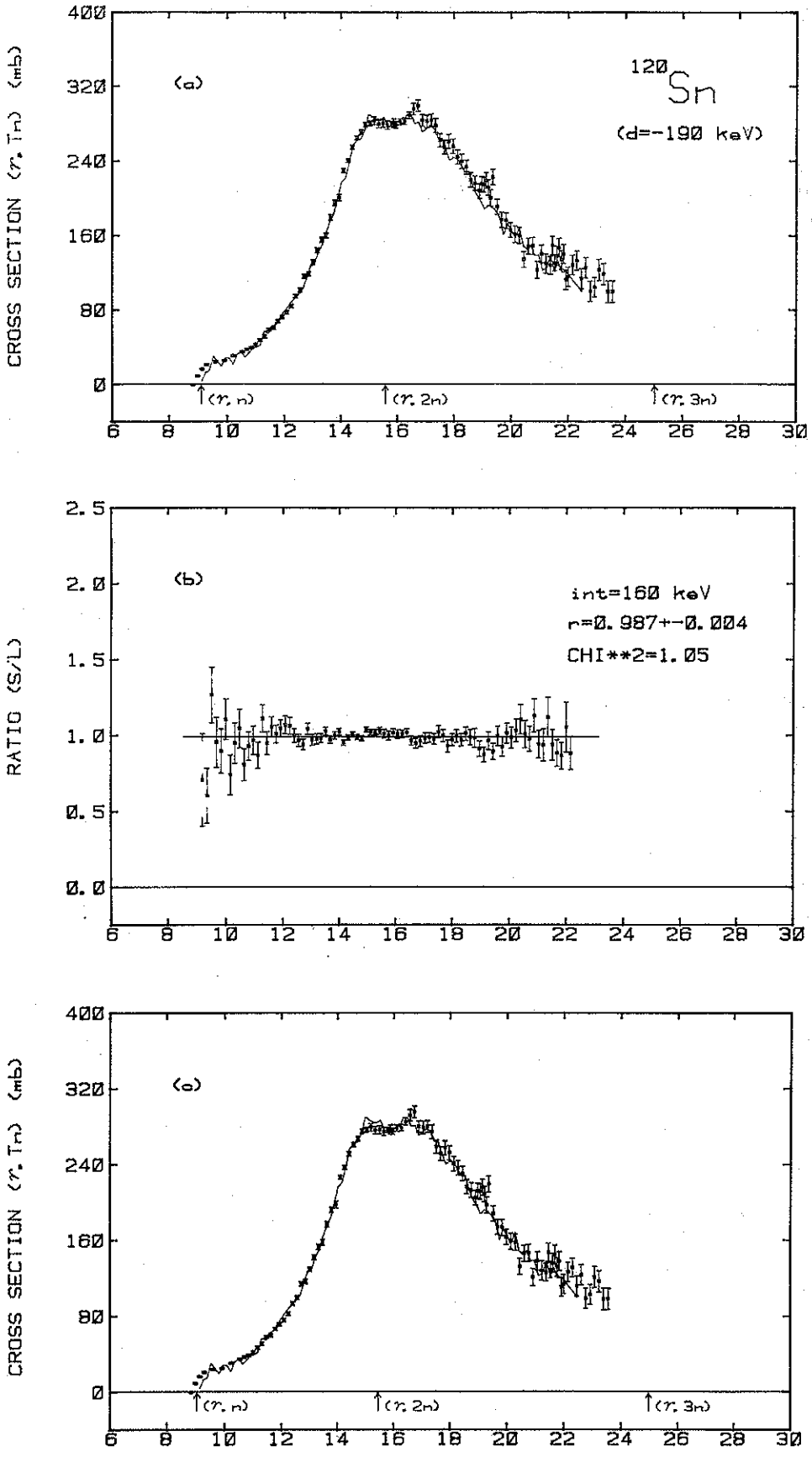
(a)
120Sn
(d=-190 keV)
CROSS SECTION (γ,Tn) (mb)
(γ,n)
(γ,2n)
(γ,3n)
(b)
int=160 keV
r=0.987+-0.004
CHI**2=1.05
RATIO (S/L)
(c)
CROSS SECTION (γ,Tn) (mb)
PHOTON ENERGY (MeV)

FIG. 19

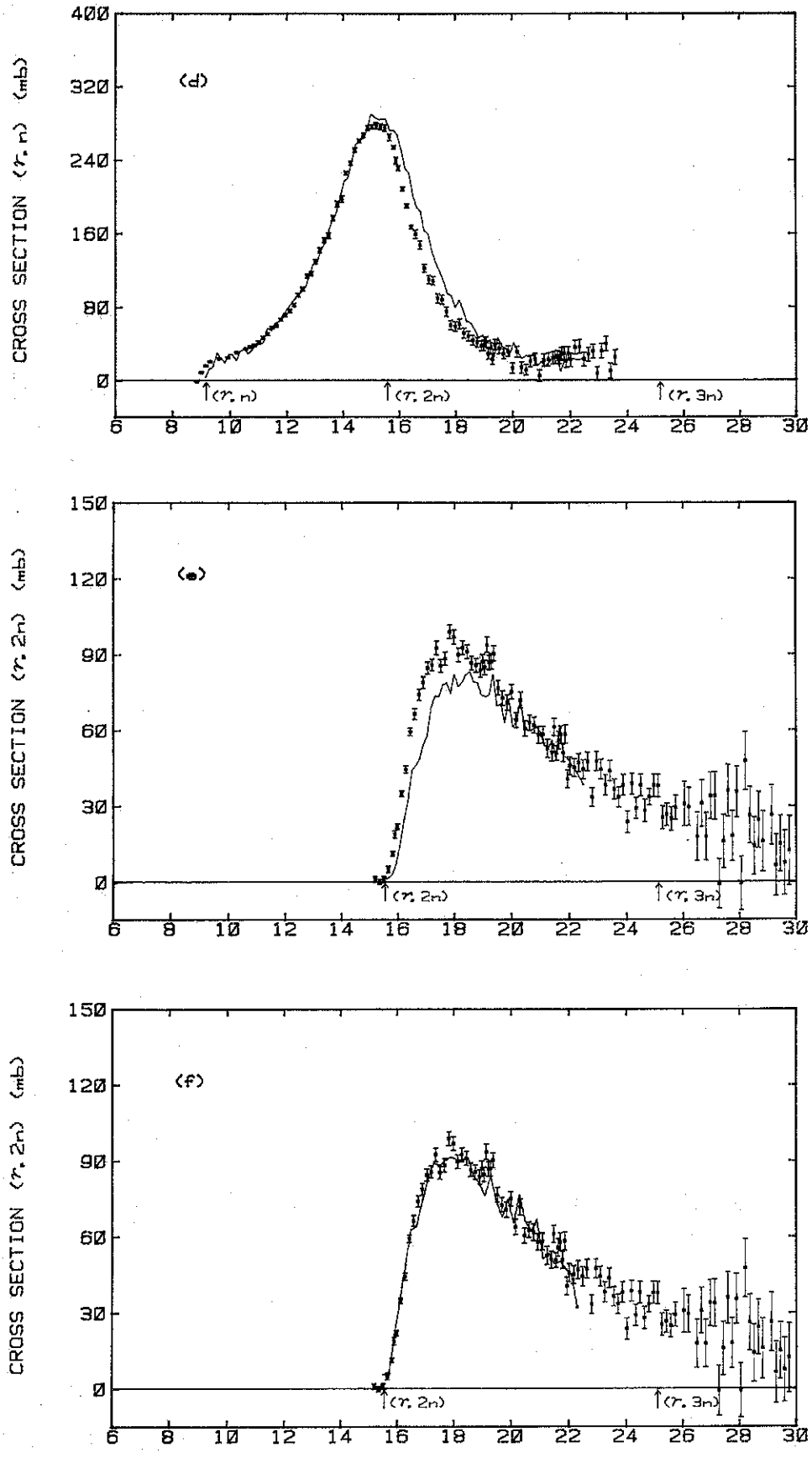
(d)
CROSS SECTION (γ, n) (mb)
400
320
240
160
80
0
(γ, n)
(γ, 2n)
(γ, 3n)
6 8 10 12 14 16 18 20 22 24 26 28 30
(e)
CROSS SECTION (γ, 2n) (mb)
150
120
90
60
30
0
(γ, 2n)
(γ, 3n)
6 8 10 12 14 16 18 20 22 24 26 28 30
(f)
CROSS SECTION (γ, 2n) (mb)
150
120
90
60
30
0
(γ, 2n)
(γ, 3n)
6 8 10 12 14 16 18 20 22 24 26 28 30
PHOTON ENERGY (MeV)

FIG. 19

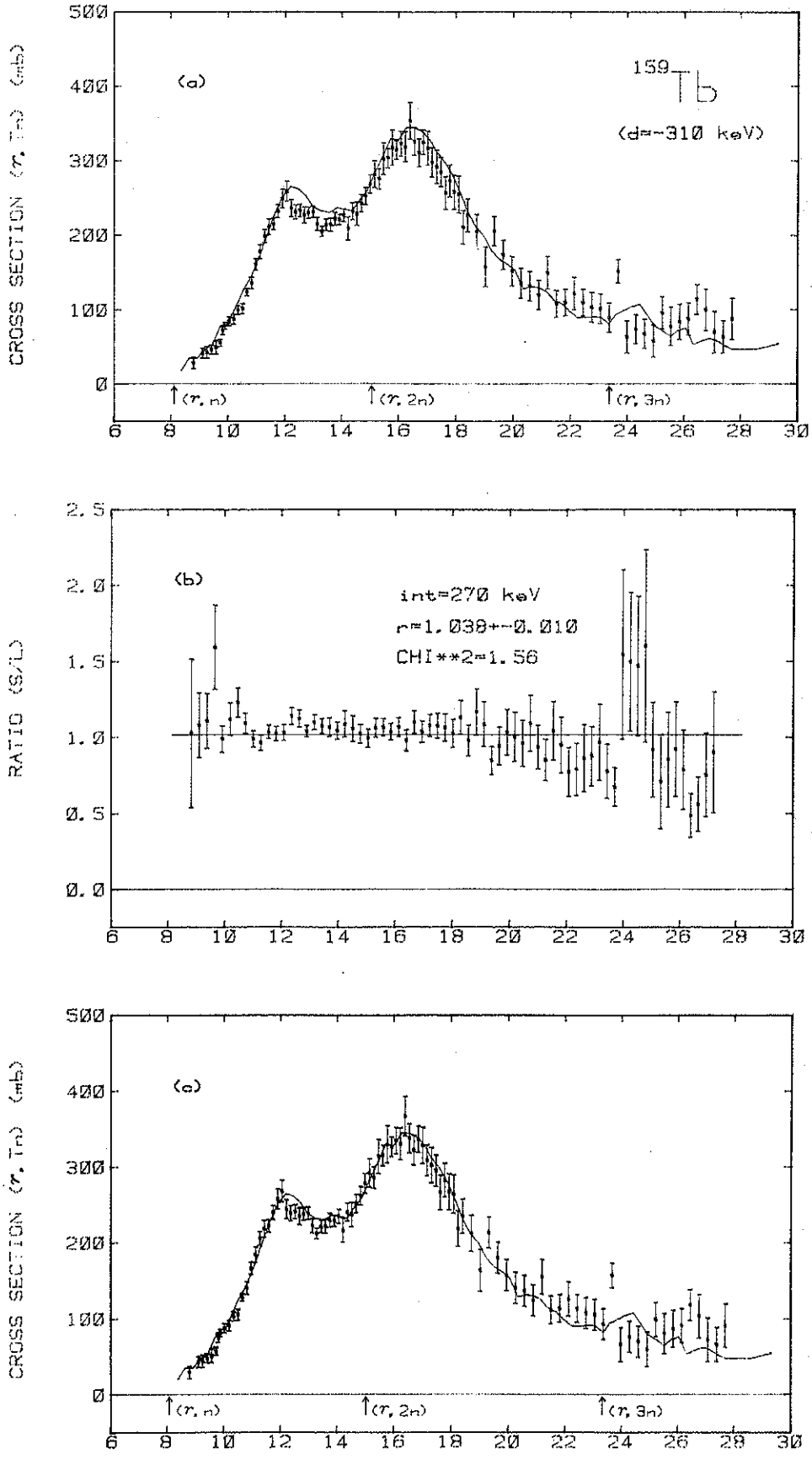
CROSS SECTION (γ, Tn) (mb)
500
400
300
200
100
0
(a)
159Tb
(d=-310 keV)
↑(γ, n)
↑(γ, 2n)
↑(γ, 3n)
6 8 10 12 14 16 18 20 22 24 26 28 30
RATIO (S/L)
2.5
2.0
1.5
1.0
0.5
0.0
(b)
int=270 keV
r=1.038+-0.010
CHI**2=1.56
6 8 10 12 14 16 18 20 22 24 26 28 30
CROSS SECTION (γ, Tn) (mb)
500
400
300
200
100
0
(a)
↑(γ, n)
↑(γ, 2n)
↑(γ, 3n)
6 8 10 12 14 16 18 20 22 24 26 28 30
PHOTON ENERGY (MeV)

FIG. 20

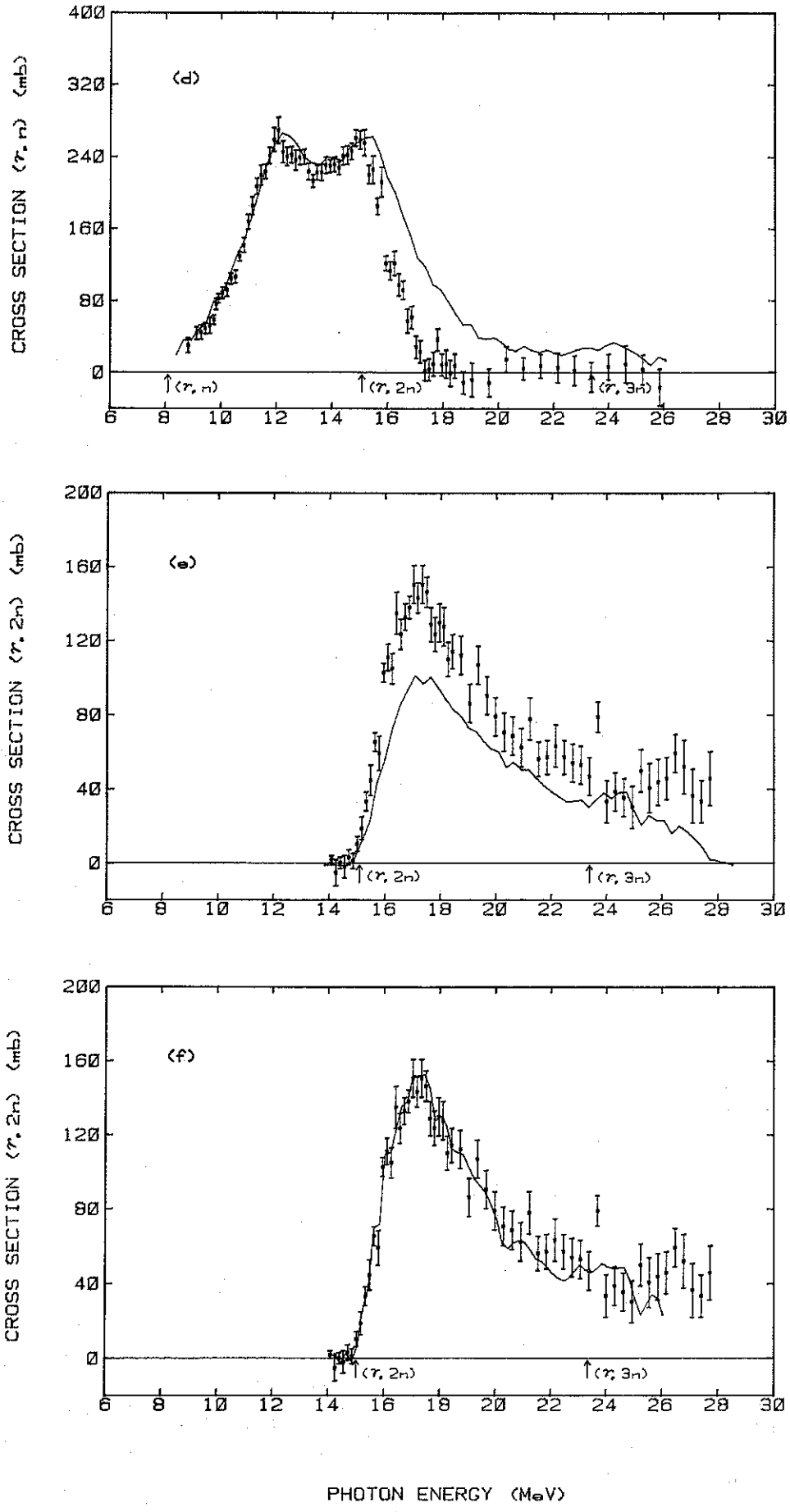
(d)
(e)
(f)
CROSS SECTION (γ, n) (mb)
CROSS SECTION (γ, 2n) (mb)
CROSS SECTION (γ, 2n) (mb)
(γ, n)
(γ, 2n)
(γ, 3n)
PHOTON ENERGY (MeV)

FIG. 20

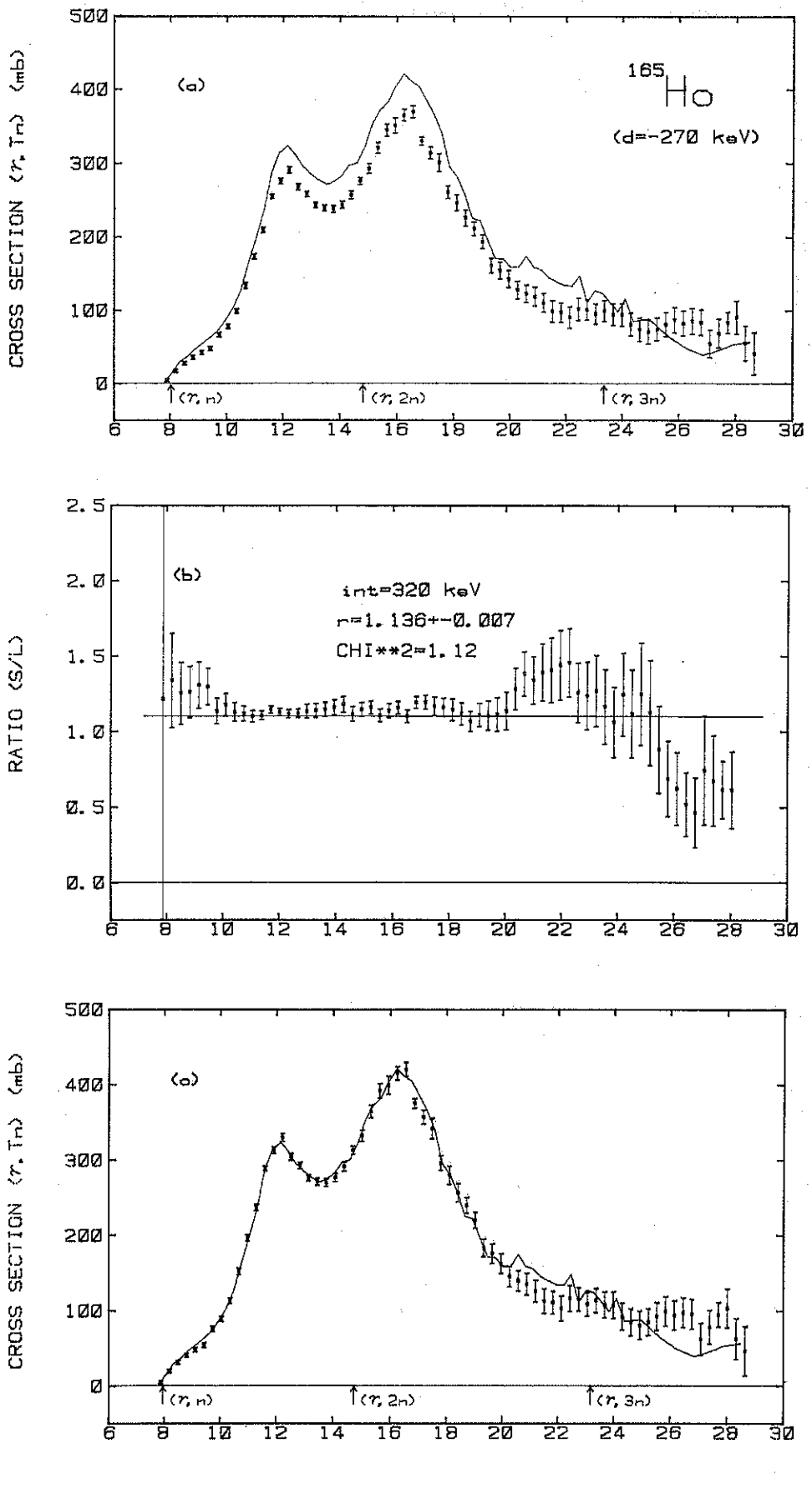
(a)
165 Ho
(d=-270 keV)
CROSS SECTION (γ, Tn) (mb)
(γ, n)
(γ, 2n)
(γ, 3n)
(b)
int=320 keV
r=1.136+-0.007
CHI**2=1.12
RATIO (S/L)
PHOTON ENERGY (MeV)

FIG. 21

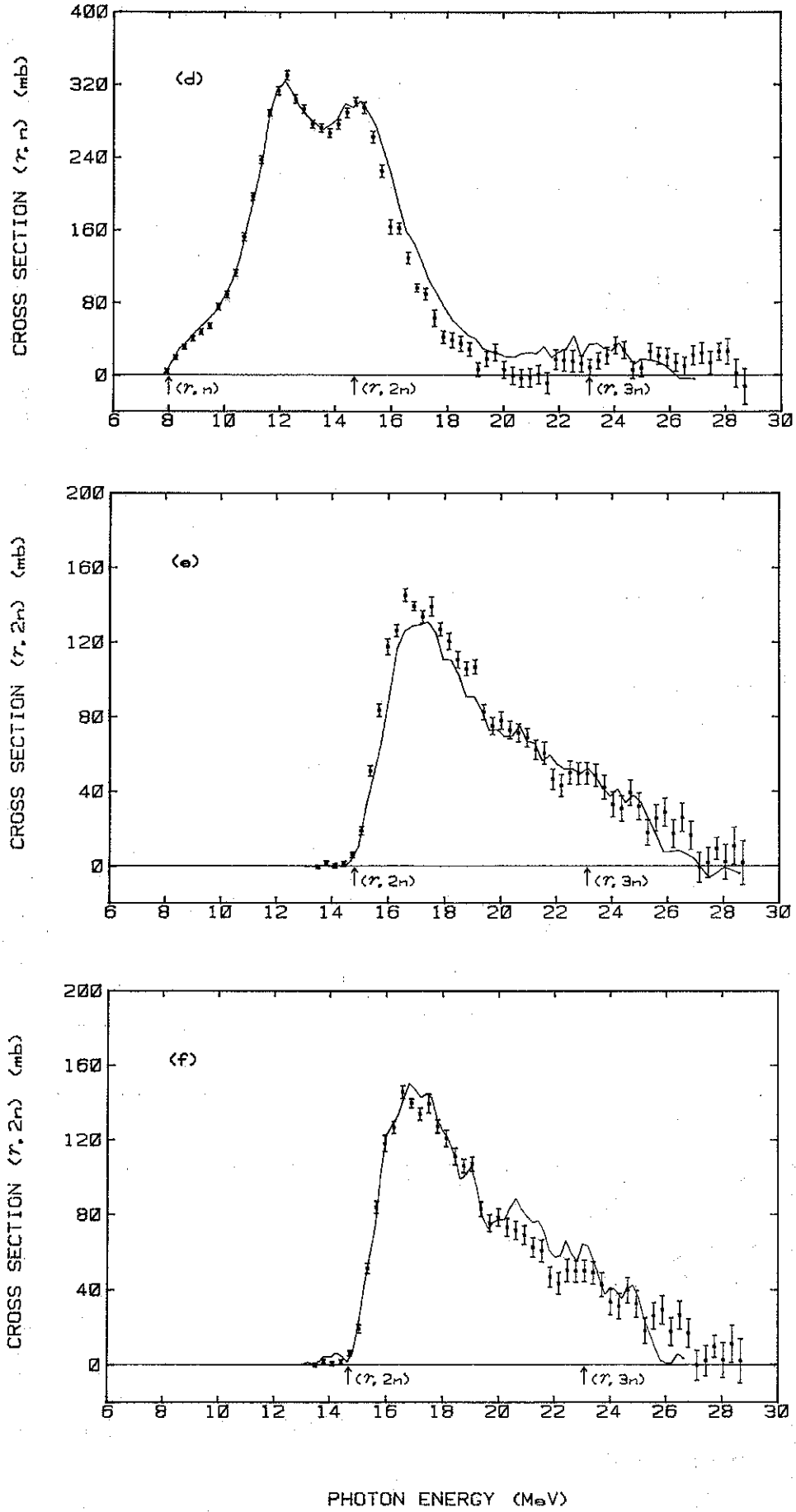
(d)
CROSS SECTION (γ, n) (mb)
400
320
240
160
80
0
(γ, n)
(γ, 2n)
(γ, 3n)
6 8 10 12 14 16 18 20 22 24 26 28 30
(e)
CROSS SECTION (γ, 2n) (mb)
200
160
120
80
40
0
(γ, 2n)
(γ, 3n)
6 8 10 12 14 16 18 20 22 24 26 28 30
(f)
CROSS SECTION (γ, 2n) (mb)
200
160
120
80
40
0
(γ, 2n)
(γ, 3n)
6 8 10 12 14 16 18 20 22 24 26 28 30
PHOTON ENERGY (MeV)

FIG. 21

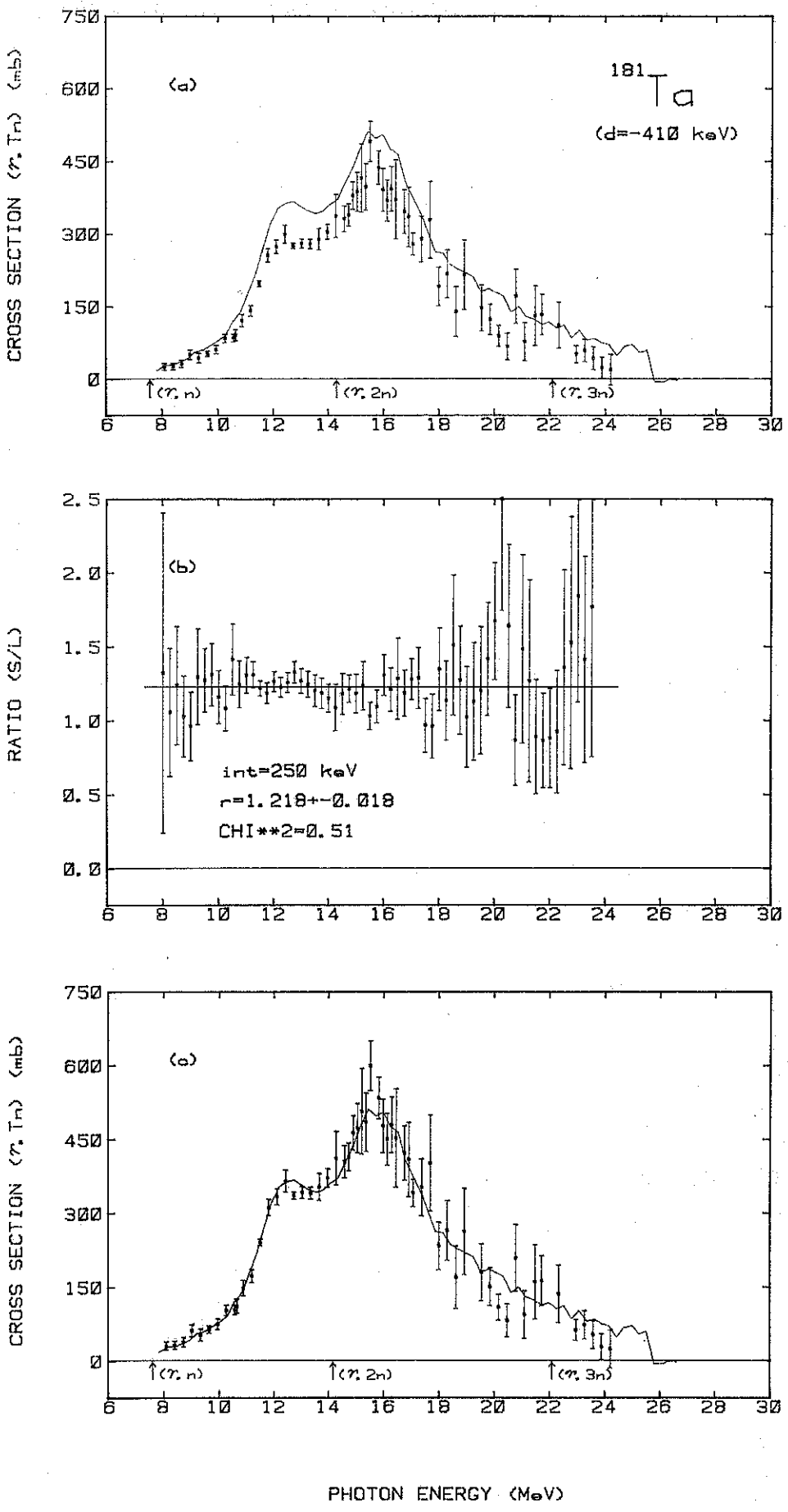
(a)
181 Ta
(d=-410 keV)
CROSS SECTION (γ, Tn) (mb)
(γ, n)
(γ, 2n)
(γ, 3n)
(b)
int=250 keV
r=1.218+-0.018
CHI**2=0.51
RATIO (S/L)
(a)
CROSS SECTION (γ, Tn) (mb)
PHOTON ENERGY (MeV)

FIG. 22

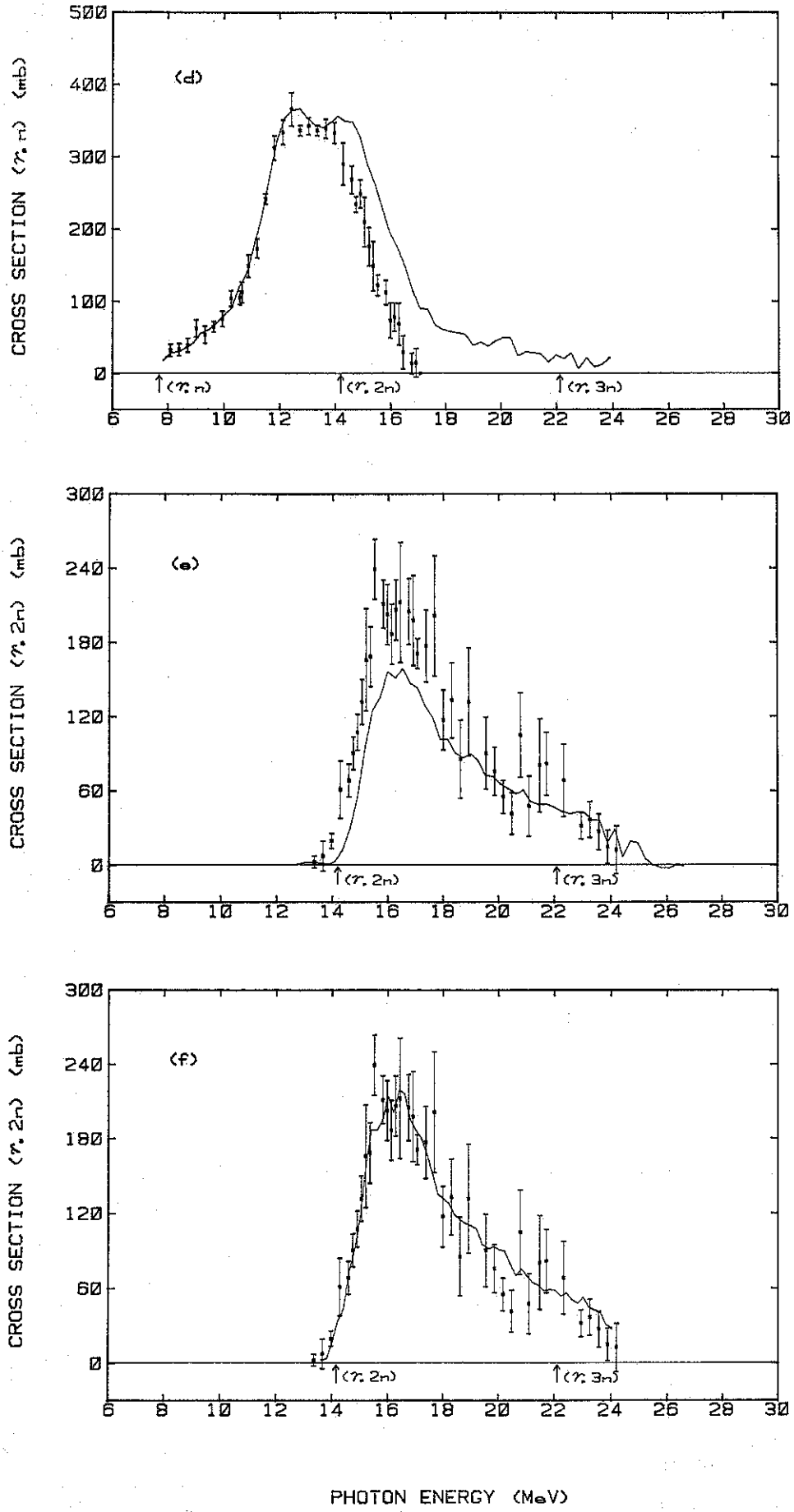
(d)
CROSS SECTION (γ, n) (mb)
500
400
300
200
100
0
(γ, n)
(γ, 2n)
(γ, 3n)
6 8 10 12 14 16 18 20 22 24 26 28 30
(e)
CROSS SECTION (γ, 2n) (mb)
300
240
180
120
60
0
(γ, 2n)
(γ, 3n)
6 8 10 12 14 16 18 20 22 24 26 28 30
(f)
CROSS SECTION (γ, 2n) (mb)
300
240
180
120
60
0
(γ, 2n)
(γ, 3n)
6 8 10 12 14 16 18 20 22 24 26 28 30
PHOTON ENERGY (MeV)

FIG. 22

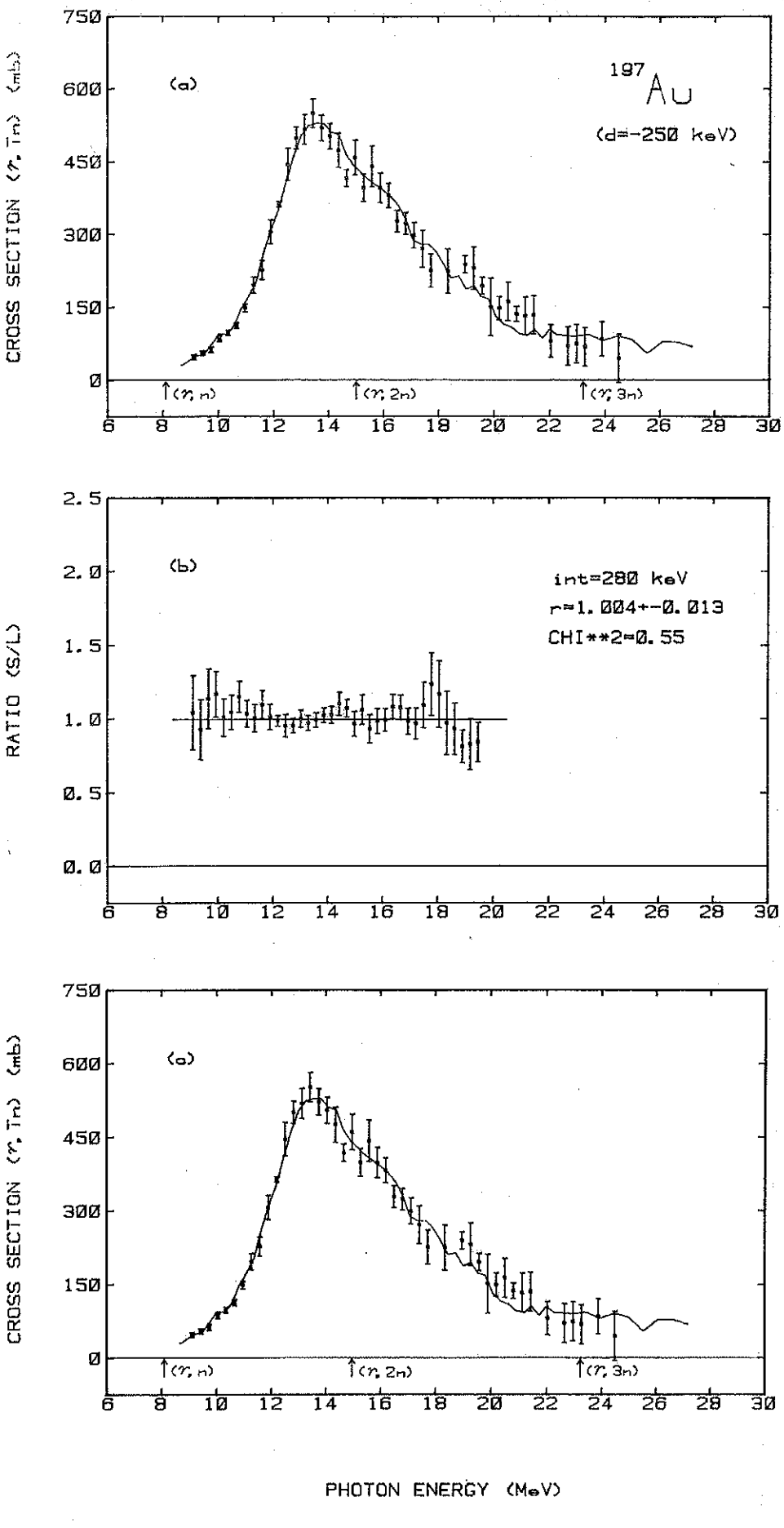
(a)
197 Au
(d=-250 keV)
CROSS SECTION (γ, Tn) (mb)
(γ, n)
(γ, 2n)
(γ, 3n)
(b)
int=280 keV
r=1.004+-0.013
CHI**2=0.55
RATIO (S/L)
PHOTON ENERGY (MeV)

FIG. 23

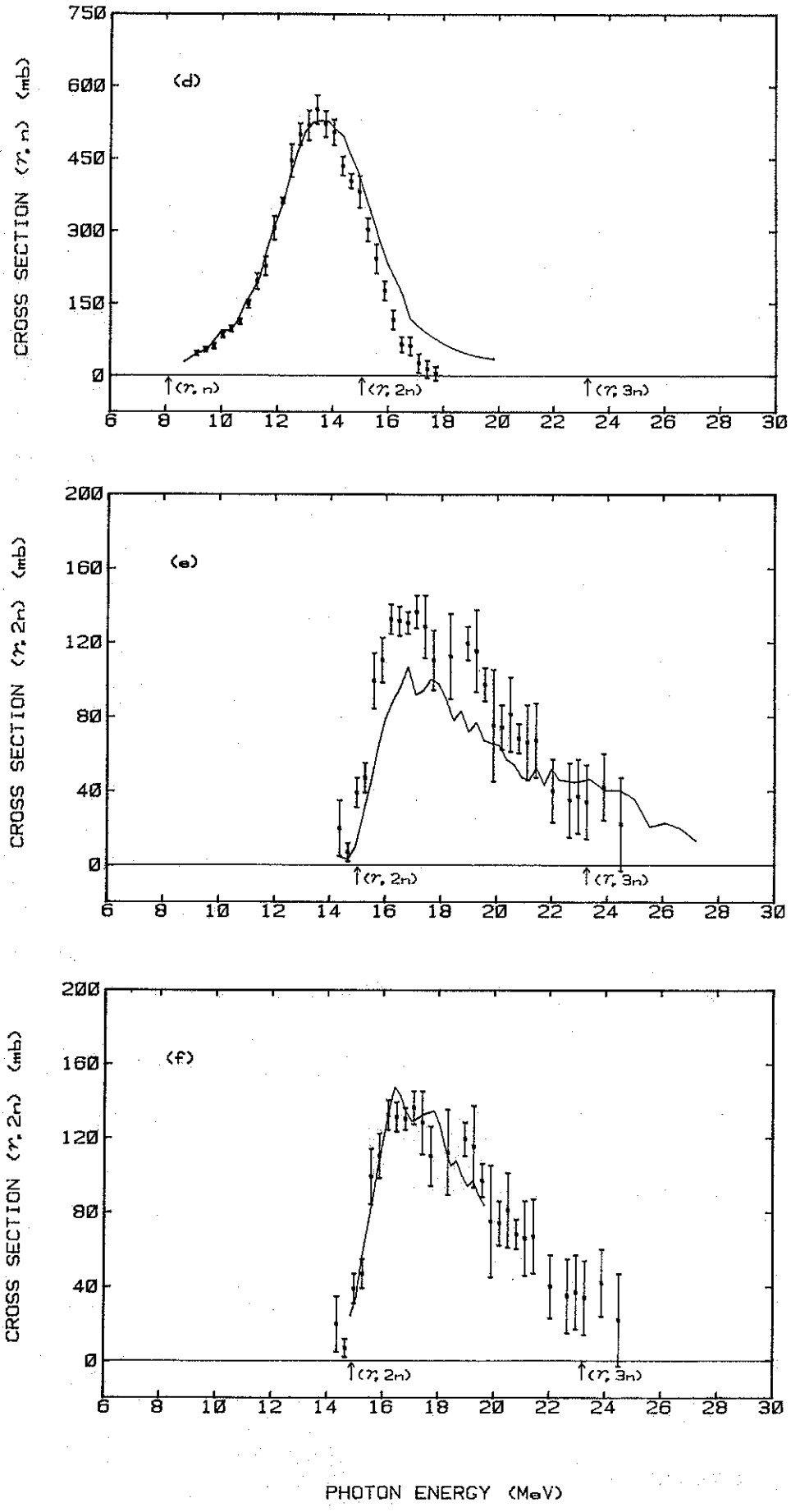
(d)
CROSS SECTION (γ, n) (mb)
750
600
450
300
150
0
↑(γ, n)
↑(γ, 2n)
↑(γ, 3n)
6 8 10 12 14 16 18 20 22 24 26 28 30
(e)
CROSS SECTION (γ, 2n) (mb)
200
160
120
80
40
0
↑(γ, 2n)
↑(γ, 3n)
6 8 10 12 14 16 18 20 22 24 26 28 30
(f)
CROSS SECTION (γ, 2n) (mb)
200
160
120
80
40
0
↑(γ, 2n)
↑(γ, 3n)
6 8 10 12 14 16 18 20 22 24 26 28 30
PHOTON ENERGY (MeV)

FIG. 23